REPORT DOCUMENTATION PAGE

AFRL-SR-AR-TR-03-

0088

1. REPORT DATE (DD-MM-YYYY)	2. REPORT TYPE	3. DATES COVERED (From - To)
28/02/2003	Final Report	01/08/2002-31/01/2003

4. TITLE AND SUBTITLE

"Identification of the Species Responsible for Biological Inactivation in the OAUGPD"

5a. CONTRACT NUMBER

F49620-02-C-0049

5b. GRANT NUMBER

5c. PROGRAM ELEMENT NUMBER

6. AUTHOR(S)

Kimberly Kelly-Wintenberg

5d. PROJECT NUMBER

5e. TASK NUMBER

5f. WORK UNIT NUMBER

7. PERFORMING ORGANIZATION NAME(S) AND ADDRESS(ES)

Atmospheric Glow Technologies, 924 Corridor Park Blvd., Knoxville, TN 37932
The University of Tennessee, Knoxville, TN 37996

8. PERFORMING ORGANIZATION REPORT NUMBER

9. SPONSORING/MONITORING AGENCY NAME(S) AND ADDRESS(ES)

USAF, AFRL, AF Office of Scientific Research, 4015 Wilson Blvd. Room 713, Arlington, VA 22203

10. SPONSOR/MONITOR'S ACRONYM(S)

11. SPONSOR/MONITOR'S REPORT NUMBER(S)

12. DISTRIBUTION/AVAILABILITY STATEMENT

Approved for public release; distribution unlimited

20030508 140

13. SUPPLEMENTARY NOTES

14. ABSTRACT

Report developed under STTR contract for topic AF0T013. Atmospheric Glow Technologies (AGT) has successfully initiated studies to elucidate the mechanims of inactivating microorganisms using the One Atmosphere Uniform Glow Discharge Plasmam(OAUGDP). AGT has worked to quanitfy the active species generated by the APD-210. The APD-210 has been independently shown to inactivate a number of different microorganisms including anthrax by convecting active species to the downstream sample. It is capable of decontaminated sensitive materiel without deleterious effects. AGT is developing plasma diagnostics to begin to understand the mechanism of inactivation of microorganisms generated by OAUGDP.

15. SUBJECT TERMS

STTR Final Report, One Atmospheric Glow Discharge Plasma, neutralization, inactivation, bacterial endospores, efficacy

16. SECURITY CLASSIFICATION OF:			17. LIMITATION OF ABSTRACT	18. NUMBER OF PAGES	19a. NAME OF RESPONSIBLE PERSON
a. REPORT	b. ABSTRACT	c. THIS PAGE			Kimberly Kelly-Wintenberg
U	U	U	UU	33	19b. TELEPHONE NUMBER (Include area code) 865.777.3776

Final Report

STTR Phase I Contract F49620-02-C-0049

"Identification of the Species Responsible for Biological Inactivation in the OAUGDP"

Contractor:

Atmospheric Glow Technologies

924 Corridor Park Blvd.

Knoxville, TN 37932

1. INTRODUCTION

The overall aim of this work effort was to develop and initiate a study to identify the active species generated by OAUGDP™ that are primarily responsible for the inactivation of microorganisms. For this project, AGT used the APD 210 (Atmospheric Plasma Device), which has been proven capable of neutralizing both biological and chemical warfare agents as well as simulants without negatively affecting sensitive equipment. AGT has recently completed an intensive study at Edgewood Chemical and Biological Center with actual chemical warfare agents. This study led by Larry Procell (ECBC) focused on byproducts produced by mustard gas, sarin, and VX upon OAUGDP exposure.

The results of Phase I work effort are discussed in this final report and will be used to further identify and characterize active species generated by the APD 210 in subsequent Phase II. The aims of the Phase I STTR are discussed below. The long term goal of AGT is to identify the OAUGDP generated active species responsible for destroying microorganisms. Once identified the system will be optimize to produce the specific active species responsible for neutralization of all microorganisms.

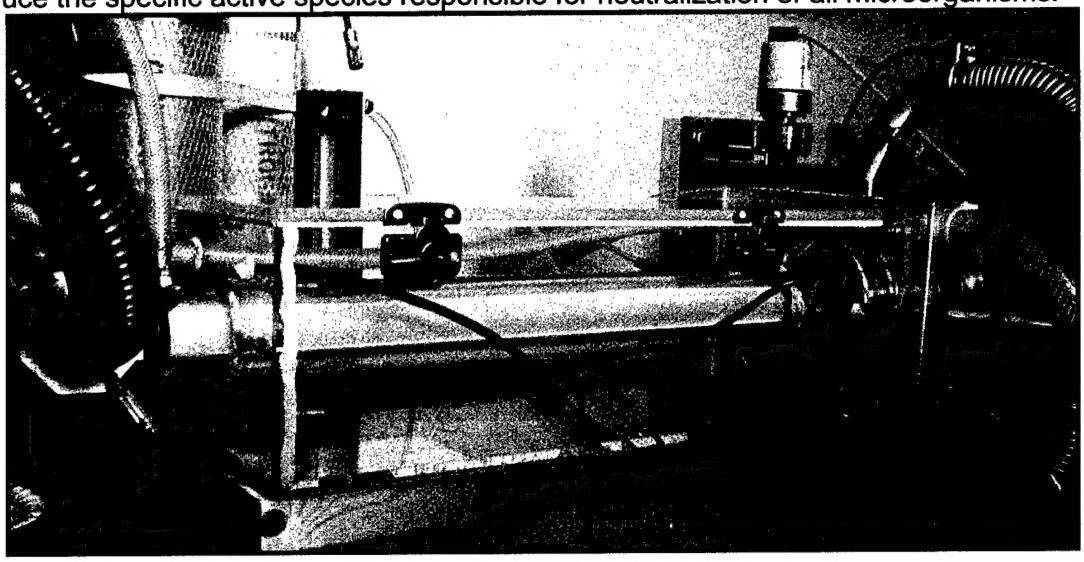

Figure 1. The APD 210 plasma device (Test Device 8) connected to the HPR-60 Spectrometer.

Aim One: Modify the APD 210 Testing Apparatus. The goal of this strategic aim was to interface the APD 210 Test Device with the HPR-60, a tripled filtered Electrostatic Quadrupole Plasma (EQP) Mass Spectrometer manufactured by Hiden Analytical, Inc. to initiate identifying the active species.

Aim Two: Verify efficacy of biological inactivation. This work was vital in ensuring that the ADP-210 reactor integrated with the HPR-60 was performing optimally such that data recorded in subsequent aims is relevant to the mechanism of inactivation. Routine biological inactivation assays were performed by AGT throughout the course of this effort to confirm that the performance of the APD 210 remains consistent. AGT's microbiologists have several years of experience in handling and processing all types of microorganisms.

Aim Three: Measure gas chemistry. Initial characterization of active species was performed with the downstream exhaust chemistry produced by the ADP-210 exhaust using the Hiden HPR-60 as well as other analytical tools. Ozone and NOx species were tracked during the studies.

Aim Four: Analyze Photon Emissions with Optical Spectrometer. Photon emissions studies from OAUGDP devices were not performed prior to the inception of this project. The photon emissions generated by OAUGD plasma were measured using a UV-Visible fiber-optic spectrometer.

Aim Five: Characterize electron populations. The chemistry of the OAUGDP is dominated by electron collisions. The University of Tennessee Plasma Sciences Laboratory (UTPSL) will participate in this effort by characterizing the electron population of the OAUGDP™. UTPSL used a sophisticated microwave network analyzer to make electron number density measurements.

Aim Six: Deliver report and prepare for Phase II. A Final Report will be submitted outlining the completion of the previous aims and the data to support our findings.

AGT has initiated the immense task of identifying variables and their relatedness that drive the generation of active species by OAUGDP. These include voltage, frequency, and current, gap distance between electrodes, electrode geometry, working gas, airflow speeds and temperature to name a few. In this study, as shown in **TABLE 1**, some of these variables were controlled while others were merely tracked and recorded. This study has provided AGT the opportunity to set up a test stand and begin to identify trends in the relationship of variables. The Phase II effort will afford AGT the opportunity to further identify, characterize and confirm those variables as well as obtain the relationships between these variables in order to produce the most efficient and cost effective decontamination tool.

2. BACKGROUND

2.1 Plasma

Plasma is often times referred to as a fourth state of matter. Plasma is a collection of gaseous molecules, atoms and electrons that, although electrically neutral overall, encompasses individually charged particles, molecular and atomic excited species, and electrons. The gas species that have not been ionized are referred to as the background gas.

Plasmas are currently used for a variety of purposes including: lighting, surface etching and deposition, and materials processing. Research in the use of plasmas for additional applications includes: sterilization, decontamination, odor control, NO_x/SO_x removal, organic contaminants destruction and surface modifications. In general, there are three types of industrial plasma discharges (going from least to greatest power): corona, glow, and arc.

2.2 OAUGDP

There are a number of ways to sufficiently energize a gas to form plasma. Relevant to the OAUGDP is RF (radio frequency) power, more specifically, capacitive RF interactions. Capacitive RF discharges imply that the energy is imparted to the electrons comprising the plasma via RF electric fields. Physically this implies that either one or both of the electrodes that the plasma forms between is covered with a dielectric/insulator, such that a real electrical current does not occur when the electrodes are energized. Displacement currents, rather than real currents, supply the power to the plasma and are responsible for less bombardment/damage/etching of the electrodes/sample by the energetic active species. Additionally, the use of RF electric fields means that the plasma is not continuously generated, but rather forms and extinguishes a number of times equal to twice the frequency of the applied voltage.

One of the key advantages of the OAUGDP is that the plasma duration is tens of microseconds for each half period of the RF cycle. When the OAUGDP is operated in air (which is the normal operating gas), the relatively long duration of the uniform plasma during each half-cycle of the RF, compared with ozonizers or dielectric barrier discharges (10–100 microseconds compared to nanoseconds), allows complex plasma chemistry to occur. This complex chemistry of the plasma results in the production of ROS that includes nitrogen oxides, ozone, species in excited and metastable states, and atomic oxygen. The mechanism of sterilization and simulant destruction observed to date is consistent with some mechanism of oxidation.

AGT has employed two modes of atmospheric plasma delivery that are based upon sample placement as shown in **Figure 2.** With **direct OAUGDP exposure (Figure 2a)**, the sample is immersed within the plasma and exposed to active species as well as ion bombardment, ultraviolet radiation, and a strong electric field. In many plasma applications, large or irregularly shaped workpieces such as sensitive materiel cannot readily fit between the electrodes of these types of atmospheric plasma reactors. To eliminate this disadvantage, AGT developed a series of reactors that allow for **indirect OAUGDP exposure (Figure 2b)**. These reactors generate potent antimicrobial active species that exit the device via the exhaust port. This ability to decontaminate without direct exposure to plasma has provided AGT extraordinary flexibility in the range of items that are compatible with this process.

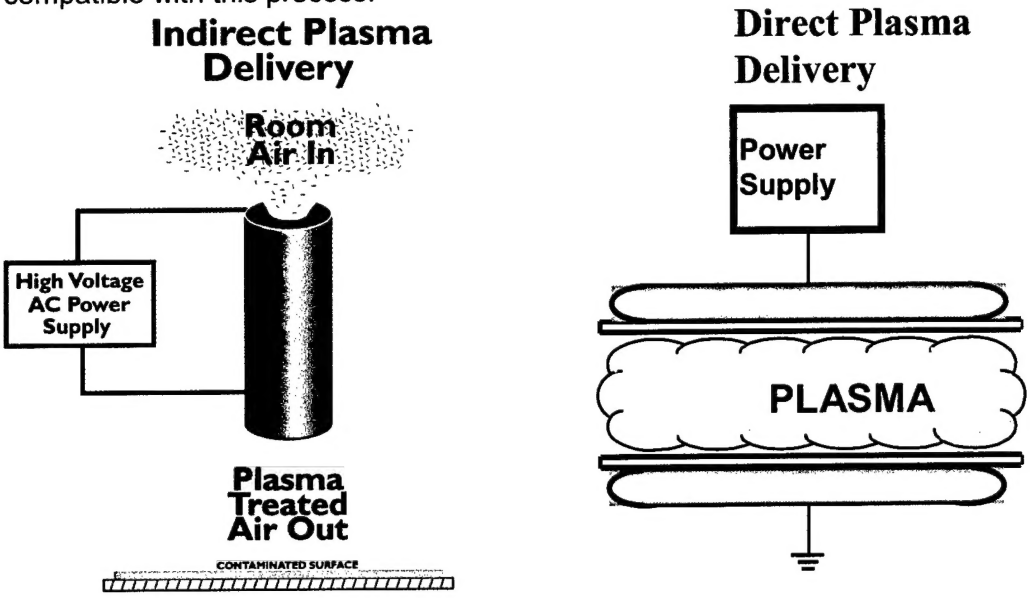

Figure 2. AGT's OAUGDP Delivery Systems (a) Indirect, (b) Direct

2.3 Biological Inactivation with Plasma

While the mechanism of inactivation of microorganisms by OAUGD plasma is not fully understood AGT is confident that the observed mechanism is generated at least in part by oxidative species produced by OAUGDP. The elucidation of the mechanism of inactivation by OAUGDP shares similarities with other biological mechanism studies in that it is difficult to separate and identify an effect on a biological cell from a single variable. In many instances one identifies and reports trends since it is difficult to decouple variables. Also in many instances there may be synergistic relationships between variable such that the desired effect is not seen when the variables are tested alone. AGT has identified a number of OAUGDP variables which include the type of devices used, the dimensions, operational regime, the power sources (frequency and voltages), the cell exposure times and locations of samples with respect to the plasma, and the plasma feed gas. Furthermore, there are numerous microbiological species that are structurally different and exhibit different levels of resistance to antimicrobials. This is one reason that AGT has used endospores as the gold standard for neutralization studies since neutralization of spores will also inactivate any other microorganism. **Table 1** describes the list of variables that were examined during the Phase I work effort.

Table 1. List of Variables Controlled or Tracked during Phase I Neutralization Tests.

Source	Variable	Range	Controlled/Tracked [1]
Feed gas/air (Indirect – APD 210)	Relative humidity Flow rate Temperature	0 – 60% 8 cfm -13.6 cfm 25 – 35 °C	C, T C T
Power supply	Voltage Frequency Power	8 – 16 kV 2 – 8.6 kHz 0.1 – 2.9 kW	C C C
Plasma device	Gap Dimensions	1.25 – 2.5 mm Test Device – 6", 22"	C C
Plasma exhaust	Ozone NO_x Temperature UV/Vis/Infr emissions	100 – 1000 ppm 0 – 600 ppm 40 – 90 °C 285 – 1400 nm	C, T T C, T T
Biological samples	Neutralization/efficacy Sample placement	10^0 – 10^6 cfu 2 – 16.5"	T C

[1]Controlled refers to variables that are manipulated. Tracked refers to variables that are recorded, but not controlled.
[2]This information will be determined for optimized operational situations during the phase II.

2.4 OAUGDP Chemistry

Plasmas are typically generated in vacuums with the consequence being reduced collision frequencies and thus simplified detection of the various species. The OAUGDP is an atmospheric plasma device (i.e. many more collisions are occurring) and also operates using air as the feed gas, thus detection of the active species becomes more difficult through the reactivity of oxygen and nitrogen. Most plasma use noble gas as opposed to nitrogen, and thus do not have the additional reactions of the gas interacting with oxygen. Additionally, other plasmas generally run with much lower percentages of oxygen, and are run dry, i.e. no humidity/water. Studies on the reactions and species in air plasma have put the number of *significant* reactions at well over 30.[1,2,3,4] Kitayama's model of ozone generation in a N_2/O_2 silent discharge (no H_2O) included 67 reactions.[1]

Directly within an air plasma are numerous species:

- Nitrogen species: N, N_2, and excited and ionized states of both
- O, O_2, O_3, and excited and ionized states of all three
- Nitrogen/oxygen species such as NO, NO_2, N_2O, NO_3, N_2O_5, as well as various excited and ionized versions of all these
- Species generated by the presence of water/humidity: H_2O, OH, H_2O_2, etc.

Of particular interest in terms of plasma and its ability to sterilize biological media are the excited and ionized oxygen species because of their reactivity and oxidative properties. Some of these species include: vibrationally excited, ground state oxygen (O_2*); excited molecular oxygen species – singlet oxygen $O_2(b^1\Sigma_g)$ and singlet delta oxygen $O_2(a^1\Delta_g)$; ground state, atomic oxygen $O(^3P)$; excited atomic oxygen $O(^1D)$; ozone (O_3); and excited state ozone (O_3*).

External to the plasma, the plasma exhaust is quite simplified in terms of the chemical composition compared to the chemistry within the plasma. Most of the species generated in the plasma are extremely short-lived (on the order of microseconds) and would therefore be reacted within a fraction of a mm outside the plasma volume. However, some oxygen species, ozone and the excited

molecular oxygen species (singlet oxygen and singlet delta oxygen), are of interest in the plasma exhaust due to their longer lifetimes. It is possible there are other active species yet unidentified that play a role in the efficacy of the OAUGDP.

The longer lifetime of $O_2(a^1\Delta_g)$ is due to the fact that, as an isolated molecule, transition to the ground state triplet O_2 is spin forbidden (not meaning that it does not occur, but that statistically and energetically it occurs much less readily than other decay pathways), and as such it is referred to as a metastable. Reported values of the lifetime of the singlet delta oxygen in pure oxygen at atmospheric pressure are 14 min.[5] Jeong and associates[6] give a lifetime of this species as 100 ms in a N_2-O_2 mix. In either case, for the OAUGDP, singlet delta oxygen should be present in the exhaust for a significant distance, dependent on the flow rate of the feed gas. In this Phase I study, the ozone concentrations in the exhaust were monitored; however, our equipment was not capable of detecting the excited molecular oxygens, particularly $O_2(a^1\Delta_g)$, which emits photons in the IR region above the range that our instruments detect.

Other species identified in the Phase I work that may possibly play a role in that decontamination include ozone and N_xO_x species. Not touched on, but also significant is the role of humidity and OH radicals produced by the plasma when the feed gas contains water. All these species must be considered as possible reactive agents, as well as their possible synergistic effects in the effort to determine the mechanism for microbial destruction. Control of the plasma and power device parameters and air feed parameters will play a role in so far as they control the chemistry of the above species.

3. APPARATUS Used in this Work Effort

3.1 OAUGDP Devices

AGT has developed a number of direct and indirect OAUGDP devices. An indirect delivery device, the APD 210 delivers plasma exhaust chemistry to remote samples as far away as 16.5". It is a cylindrical device, with an inner metal electrode and a dielectric-insulated outer electrode, which are both water-cooled as shown in **Figure 3**. This construction is used to reduce costs because a metallic coating doesn't have to be applied to the outer diameter of the dielectric comprising the outer electrode as well as providing a good way to visualize the plasma while in operation.

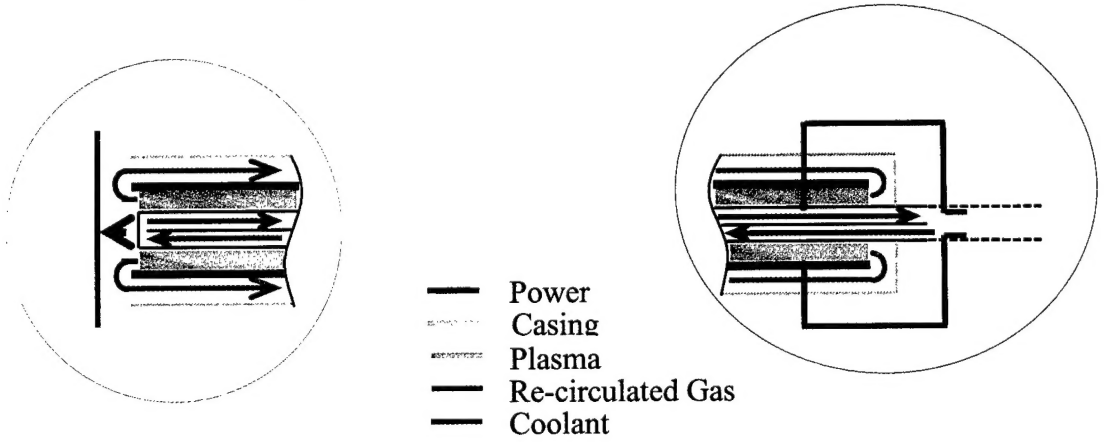

Figure 3. Schematic of APD 210 showing the components.

The energized gas flows through the air gap that is located between the concentric electrodes. Device specifications are given in **Table 2**, and a schematic of the cross-section of an APD210 is seen in **Figure 4**. Several of these devices were fabricated for this study, differing in gap size, length, and materials of construction.

Table 2. Atmospheric Plasma Devices (APD) specifications.

Device	Type	Length[1] (cm.)	Gap[2] (mm)	Inner Electrode	Outer Electrode
APD 210 B4	Test Device, single pass	58.42	2.65	316SS, or Aluminum. (1.0 in OD)	Pyrex
APD 210 B8	Test Device, single pass	55.56	1.25	316SS 2.8 cm OD	Pyrex
APD 210 B9	Test Device, single pass and recirculated	30.80	1.25	316SS 2.8 cm OD	Pyrex
APD 210 B10	Test Device, single pass	57.15	1.8	316SS 2.8 cm OD	Quartz
APD 210 B11	Test Device, single pass	14.61	1.25	316SS 2.8 cm OD	Pyrex

[1]Length refers to the actual length of plasma discharge within the device. SS-stainless steel
[2]Gap refers to the distance between the OD of the inner metal electrode and the ID of the outer dielectric electrodes.

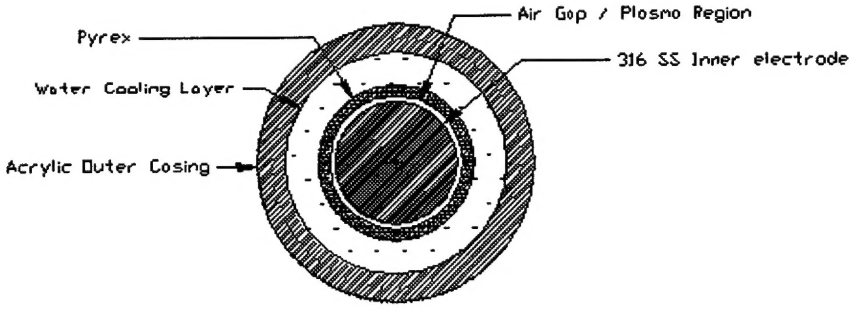

Figure 4. Cross-sectional drawing of the APD 210.

3.2 Power Supplies and Electrical Diagnostics

Power to the OAUGDP devices is provided by a high voltage power supply. In general this power supply consists of an amplifier, limited matching inductor, and transformers. Two sets of transformers were used: one for operation at the two kHz frequency and the other set for operation between 5 kHz to 10 kHz. The same power supply was used during the entire study. A schematic of the power supply and the associated electrical diagnostic equipment is shown in **Figure 5**.

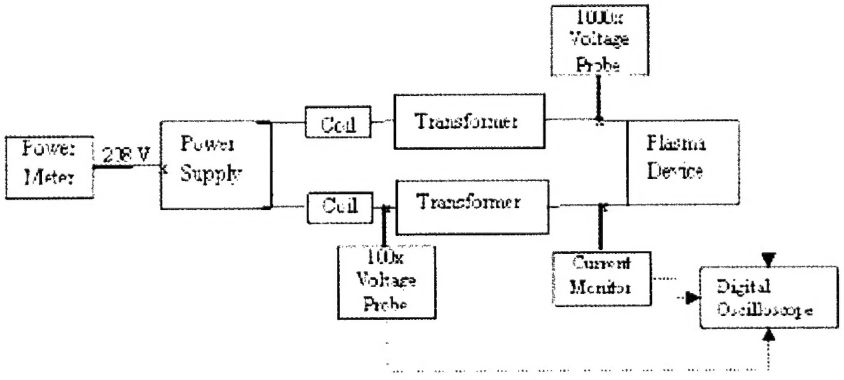

Figure 5. Components of the Electrical System.

The primary of the transformer was monitored with a Tektronix 100x voltage probe that was displayed on a Tektronix Model TDS3034 4-channel oscilloscope. The secondary of the transformer was monitored with both a 6015A Tektronix high voltage probe and Pearson Electronics model 2100 current monitor that were also connected to the oscilloscope. The input the power supply was monitored with a portable Fluke, Model 39 digital power meter.

3.3 Airflow Handling and Cooling Equipment

Room air was pushed through the APD 210 device using a Gast Idex, Inc. model R3105-12 ring compressor blower. This blower has an open airflow rate of 53 cfm, and a max pressure of 55 inches of water. Commonly the blower was choked down via a valve to operate around 10 cfm. The flow rate of the blower was monitored using an airflow orifice made by Lambda Square serial no. 21981. The airflow orifice was read via a magnehelic. The devices were calibrated using a common rotameter flow meter. The purpose of maintaining and relatively increasing/decreasing specific flow rates was accurately achieved. The temperature of the airflow was monitored beside the sample using a thermocouple. The air temperature was adjusted by placing a heater coil either in the inlet or exit of the plasma device.

The current laboratory versions of the APD 210 are water cooled. The water was provided by a Neslab water chiller, model HX+300w/c. The water was delivered to the APD 210's at 40 psi at a constant temperature ranging between 5 to 37 degrees Celsius. Due to the water being in contact with both the high voltage electrodes, both the supply and the return of the water from the plasma device was passed through a set of water coils to drop any accumulated charge in the water, this insured the safety of both the operator and cooling equipment. In most of the later experiments, the water chiller was actually set to heat the water to 37 degrees. The chiller temperature setting had a significant affect on the temperature of the plasma exhaust gas because of the large surface area of the electrodes in contact with the relatively smaller volume of air feed gas/plasma.

3.4 Qualitative Spectral Devices

3.4.1. Sampling Gas Analysis System

The HPR-60 is a triple filtered Electrostatic Quadrupole Plasma (EQP) Mass Spectrometer (MS) manufactured by Hiden Analytical, Inc., was purchased by AGT in October of 2002. It has an attached molecular beam sampling system designed specifically for the study of both stable and reactive species, including ions, neutrals and radicals. During the Phase I effort it was used to qualitatively determine the active species present in the exit gas from the plasma reactor. In addition to mass determinations, the HPR-60 was used to differentiate species with the same m/z ratio according to their electron energy potentials. The species can be differentiated via a built-in selectable electron energy source. The HPR-60 was interfaced to the plasma device via an acrylic sample chamber.

3.4.2. Spectrophotometers

Three different spectrophotometers, models of Stellarnet's EPP2000 for UV, Vis, and Infrared spectrum were daisy chained together and interfaced with the plasma devices. For different chemical reactions within the plasma, photons are emitted at specific wavelengths. These light emissions facilitate an additional indication of neutral, excited, and charged species within the OAUGDP exhaust. **Table 3** describes the features of the spectrophotometers.

Table 3. EPP2000 features for the UV/Vis/Infrared Spectrometers

	UV2	Vis-25	Infrared(NIR2B-25)
Spectra Range (nm)	200-400	380-780	780-1180
Slit size (micron)	25	25	25
Grating (g/mm)	2400	1200	1200
Resolution (nm)	< 0.5 nm	< 0.5 nm	<0.5 nm
Multi-beam architecture			
IEEE 1284 Digital Interface			
No moving parts or mirrors			
Temperature controlled			

3.4.3 Quantitative Gas Monitoring Devices

Quantitative measurements of the plasma exhaust gases were made with ozone and NO_x monitors. These were chosen because of ease of use and indicators of performance of Test Devices when variables were modified. Changes in the concentrations of either would trigger a more in depth evaluation. This however was not the only criteria to trigger further studies merely a piece of the puzzle. This was The ozone monitor is an Advanced Pollution Instrumentation (API) Model 450 - Nema with a range of 0.003 ppm to 1000 ppm by volume ozone determination (accuracy is 0.5% of reading). Nitrogen oxides, specifically NO and NO_2, were monitored within the plasma exhaust using API's Model 501 NO thermal converter and chemiluminescent NO_x Analyzer Model 200AH that has a range of 0.05 to 5000 ppm +/- 0.5%. The sample intake lines were located within the plasma exhaust plume and adjacent to the biological spore sample strips.

The temperature probes, thermocouples, were also interfaced with the device exhaust. The thermocouples were connected to a Fluke 50D k/j 2 channel thermometer which was located in such a manner to prevent any electrical interference that might have been generated by the plasma. The probes, again, were located adjacent or directly above the biological spore sample strips. Room temperatures were recorded for reference. The relative humidity of the room was recorded and referenced where needed for comparison purposes only.

4 EXPERIMENTAL OVERVIEW

4.1 General Experimental Setup

The devices described above were interfaced with the APD system testing apparatus. A schematic of the complete system is shown in **Figure 6** and a photograph of the APD 210 and test chamber connected to the HPR-60 was shown in **Figure 1**. Near the completion of Phase I, an Agilent model 34970A digital acquisition was installed and interfaced into the testing apparatus to assist in data collecting from different diagnostic devices.

4.2 General Experimental Procedures

A sample chamber was constructed such that a plasma device was placed at one end and the biological sample was placed at the other end, where the analytical measurements were also made. A 2-D schematic of the experimental setup is shown in **Figure 7**. Because of the airflow rates through the test devices, an exhaust plume was formed. When a single spore sample was exposed to the exhaust it was placed in the center of the plume. In several cases, multiple samples were exposed and their placement is reported.

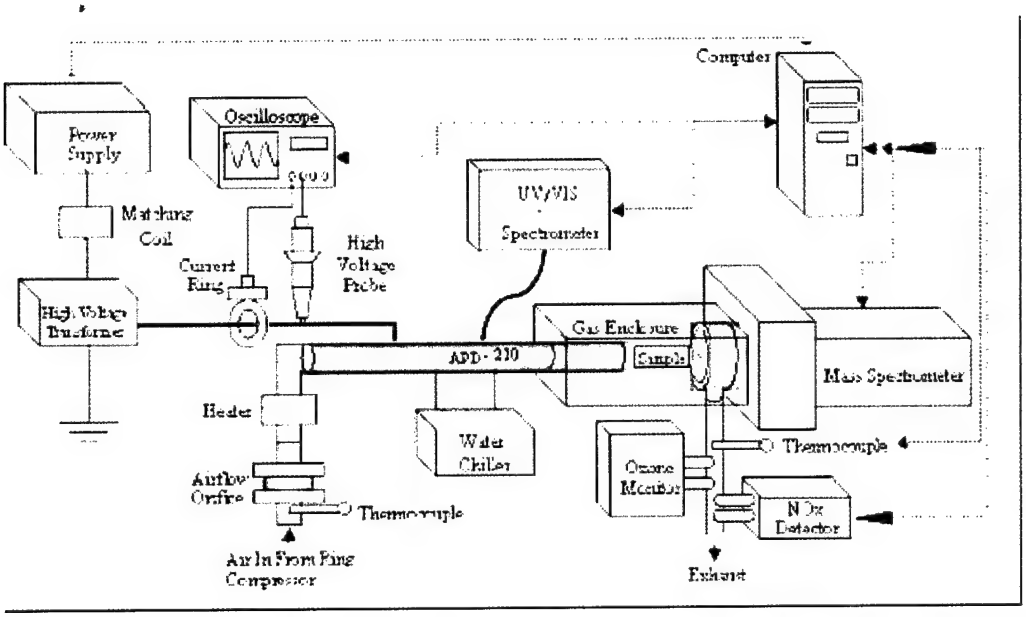

Figure 6. Schematic of the Complete Experimental Setup with the APD 210 Test Device.

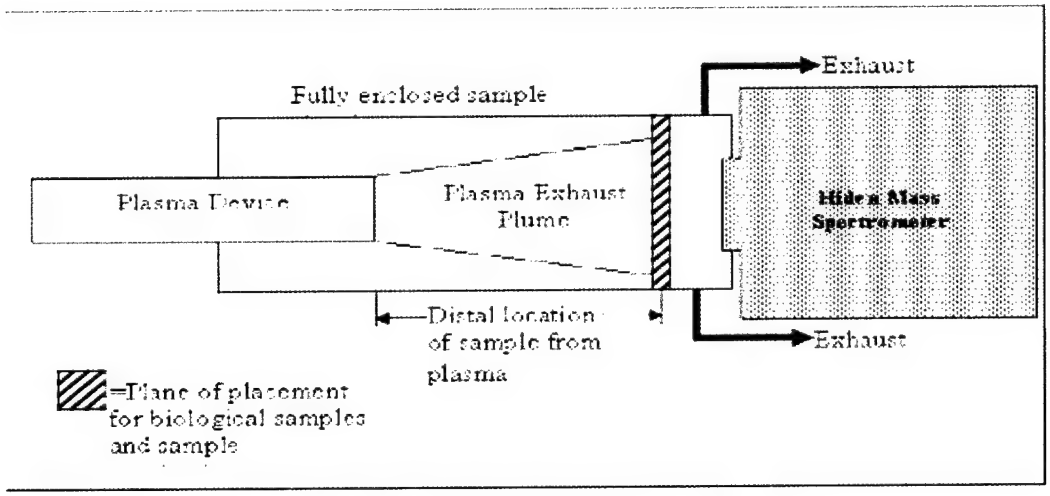

Figure 7. 2-D Schematic of the Sample Exposure Chamber.

4.3 Summary of the Evolution of the Experimental Testing

APD 210 development is an ongoing effort being performed by AGT with support form a DoD Army SBIR Phase II contract. An important developmental milestone has been reached when the gap distance between the electrodes was reduced. This change alters the surface to volume ratio, thus improving i.e. lower the average exhaust temperature coming from the Test Device. Another benefit is the reduction of plasma volume and power required to run the device.

Spectral identification software, consulting the NIST data library, and doing a comparison of spectra with other gases aided identification of the spectral peaks being observed by the spectrophotometers. The resulting identification of the spectral information is discussed in the results section.

The HPR-60 is an advanced gas diagnostic tool that has several modes of operation – positive RGA, negative RGA, and SIMS. The modes of operation have shown a wealth of information and much work to be done to assemble the complete picture.

4.4 Assessment of Biological Inactivation

Bacillus subtilis variant *niger* (recently designated *B. atrophaeus*, ATCC 9372) endospores were purchased from North American Science Associates as spore strips. Following OAUGPD exposure, the strips are homogenized in sterile buffered solution containing a mild non-ionic detergent for 4 min. Standard dilutions and plate counts are performed, and the number of survivors was determined after a minimum of 72 h incubation. Endospore samples were processed and plated in duplicate or triplicate. Controls included samples not exposed to the plasma device, or those exposed to an equivalent airflow in the absence of a plasma.

5 RESULTS

The definitive measure of success of this work effort was neutralization of endospores achieved by the APD 210 test devices. However, the OAUGDP exhaust chemistry was also evaluated for a range of variables to initiate the identification of the active species. Consequently, the results section offered here is divided between observed trends in OAUGDP exhaust chemistry production as a function of input system variables and efficacy study results produced by the test devices. When taken together, these findings will establish the requirements for constructing appropriate experiments for the Phase II proposal. Furthermore, this section fulfills the Aims 1-4 of the proposed Work Plan.

5.1 Characterization of Chemistry

The chemistry results have been compiled by three separate measurement methods: 1) use of the HPR-60 EQP-MS Analyzer by obtaining basic mass scans and electron energy scans, 2) ultraviolet/visible/infrared spectrophotometer measurements, and 3) direct measurements of particular gases and temperature of the chemistry flow stream. The first two measurement methods provide qualitative results whereas the third method offers quantitative values. The overall results of these measurements indicated that the plasma devices produced a complex chemistry and further, the relationships between the various parameters that define the plasma were nonlinear and will demand a detailed analysis to fully comprehend them.

5.1.1 HPR-60 EQP-MS Analyzer Measurements

For the Phase I effort, only a limited amount of data was obtained by the HPR-60 EQP device. The comprehensive nature of the device requires extensive training and operations experience. The machine was obtained late in the project period thereby limiting its contribution to information. Although, the range of the EQP MS device will allow extensive information to be obtained in future work.

5.1.1.a Basic Mass Scans

Analyses of the plasma exhaust chemistry using the EQP MS began with basic mass scans. A comprehensive look at the mass scan of plasma exhaust chemistry was completed initially on the APD 210 Test Device 10. Baseline runs were completed (airflow only) to compare with the exhausted air from a plasma reactor. **Figure 7** shows the signals obtained for specific masses of interest in the baseline case and plasma exhaust chemistry at applied voltages of 10 kV and 13 kV (2 kHz-APD 210 Test Device 10). Note that the signal is only qualitative, and does not convert directly to concentrations of species present. Calibrations would need to be run with the specific gas to obtain quantitative numbers. **Figure 7** shows trends for the given species in the plasma exhaust chemistry as compared to airflow only.

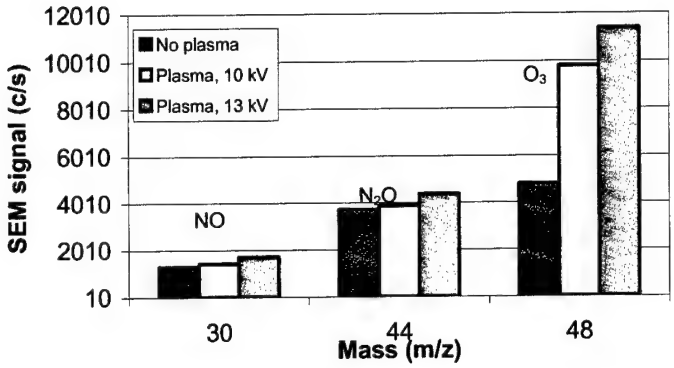

Figure 7. Qualitative signal from the EQP for masses of interest (m/z=30, 44, and 48[x10^2]) for the baseline case -no plasma- and plasma exhaust from the APD210 Test Device 10 at applied voltages of 10 kV and 13 kV (both at 2 kHz).

5.1.1.b Electron Energy Scans

Electron energy scans of NO and NO_2 were made while using several plasma devices operated at different voltages and frequencies. All runs were made in two modes, background and "plasma on". Some variance in signal output (counts/sec, c/s) is attributable to the temperature difference between plasma exhaust chemistry and background, airflow only. Temperature controlled backgrounds will be examined in future work. Preliminary results of the electron ionization potential for NO (m/z of 30) are shown in **Figure 8**. The feature of note in this figure is the additional "hump" or ionization potential at approximately 42-46 eV for the plasma exhaust of APD210 Test Device 8, yet not shown in the APD 210 Test Device 10 exhaust chemistry. This additional potential indicates a species of NO in the Test Device 8 plasma exhaust chemistry that is not present in either the background or Test Device 10 exhaust chemistry. This NO may be a fragmentation from a product of the Test Device 8 plasma exhaust chemistry (i.e. NO_2,N_2O, N_2O_5) or metastable form of NO. Currently, no match of the reported ionization potential has been made with values reported in literature.

Accumulated scans at m/z=46 show an additional species is present in the plasma exhaust with m/z equal to 46. Background and plasma scans for this situation are shown in **Figure 9**. At this time no conclusions have been reached as to the speciation of this ion. Further analysis at this mass in the secondary ion mode will clarify whether the species exists as a charged particle external to the spectrometer. Clarification concerning the origin of the species will be sought, as the possibility exists that it is a fragment from another N_xO_x form.

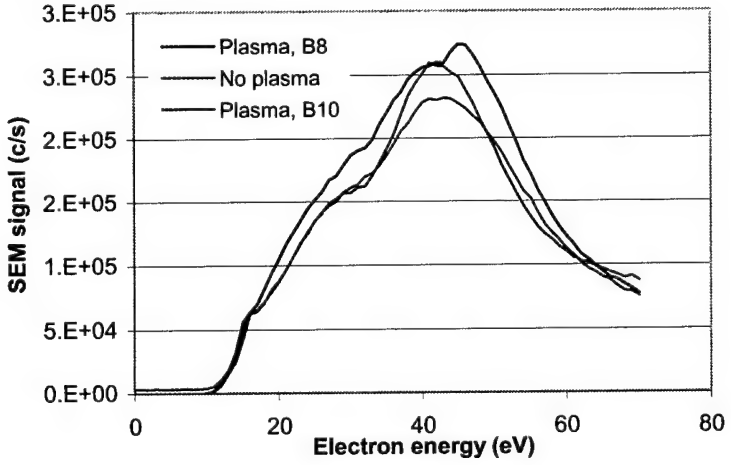

Figure 8. NO (m/z=30) accumulated electron energy scans for plasma exhaust from APD210 Test Device 8 at 14 kV, 6kHz; APD210 Test Device 10 at 12.8 kV, 5 kHz; and background (no plasma). (Plasma device located ~3" from EQP). (ref. exp. 9 & 10)

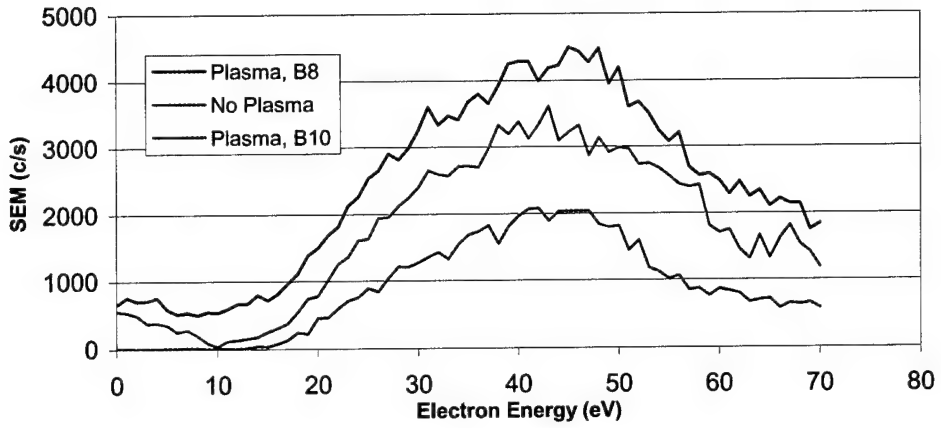

Figure 9. Accumulated electron energy scan for NO_2 (m/z=46) for plasma exhaust from APD210 Test Device 8 at 14 kV, 6kHz; APD210 Test Device 10 at 12.8 kV, 5 kHz; and background (no plasma). (Plasma device located ~3"from EQP) (ref. exp. 9 & 10)

Scans of the electron energies at m/z=16 in the negative RGA mode have shown a species of oxygen to be formed through ionization within the EQP MS of the entering plasma exhaust chemistry sample. **Figure 10** shows the accumulated electron energy scan (and baseline scan) for a n exhaust chemistry sample resulting from the APD 210 Test Device 10 operated at 12kV and 5.8kHz. The baseline case was heated air, no plasma (but at the same temperature and velocity as the plasma exhaust chemistry). The plasma curve clearly shows an additional peak at about 3.9eV that is not present in the baseline case. This peak is likely the result of the ionization of O radical resulting from the destruction or fragmentation of ozone, either external to the device or within the MS.

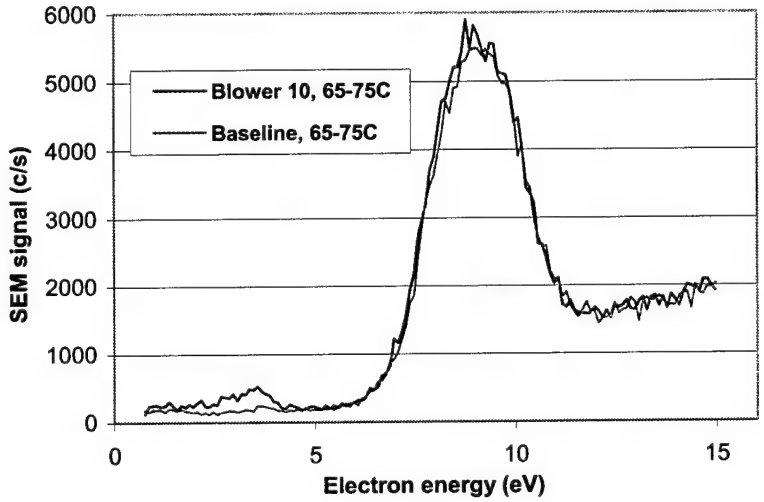

Figure 10. Accumulated electron energy scan for O (m/z=16, negative ion mode) plasma exhaust chemistry from APD210 Test Device 10 applied voltage of 12 kV, 5.8 kHz.

5.1.2 UV/Visible/Infrared Spectroscopy

An ultraviolet/visible/infrared spectrophotometer has been interfaced with several plasma devices. Copious amounts of information have been collected in the form of spectra in these electromagnetic regions. Many peaks are seen in the UV range, suggesting a lot of activity with electron energy levels. The visible spectra of the plasma devices show several peaks as well, although at lower intensities. The near infrared and infrared regions, which correspond to energy photons emitted by changes in rotational energies, are less active to the range we were able to observe. **Figure 11** is an

example of a UV spectrum obtained for increasing voltages, for the single-pass APD-210B9 at 2 kHz. **Figure 12** is corresponding visible region spectrum for the same device.

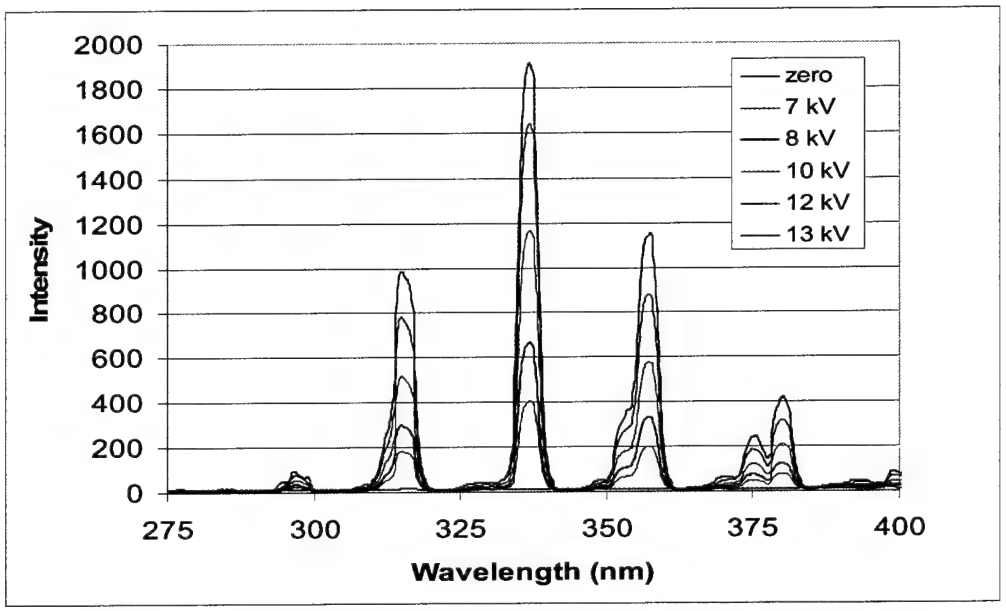

Figure 11. UV spectra of 2 kHz plasma in APD-210 version 10 with 9.63 cfm.

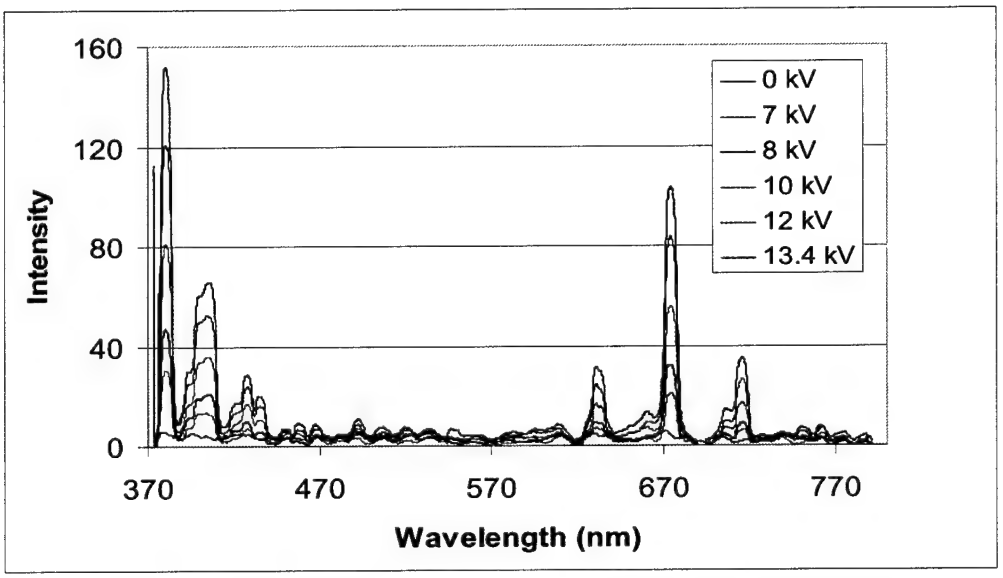

Figure 12. Visible spectra for 2 kHz, 8 kV plasma in APD-210B9 device.

While there are many possible ionic species that would have spectral emission lines in the UV-Vis regions including nitrogen, oxygen, and argon ions and neutrals as well as a few molecules (NO, NH, and O_2) . **Tables 4 and 5** list the species and their corresponding emission peak wavelengths in the UV and visible regions, respectively.

Table 1. Possible species in air plasma and corresponding peak wavelengths in the UV region.

Species	Wavelenth (nm)	Species	Wavelenth (nm)
Ar I	357.23	N II*	314.99
Ar II	357.20 375.29	N III	336.74 375.26
Ar II *	314.99 380.32 393.00 399.48 406.29	O II*	336.70 375. 380.31 406.29
H_2*	375.19 380.30 406.24	O_2^+	297.00
N I	357.20	NH	375.
N II	393.04 399.5	NO	367.24

Table 2. Possible species in air plasma and corresponding peak wavelengths in the visible region.

Species	Wavelenth (nm)	Species	Wavelenth (nm)
Ar I	750.07	O I*	406.05 467.30
Ar II	715.30 761.80	O II	427.31 467.20
N I	427.33 673.69	O II*	406.05 434.74
N I*	434.67 448.20 467.31	O III	673.93
		NO_2	630.50

As mentioned previous, by purchasing a spectrum-identification program, and consulting the NIST online data base, the spectra observed in **figures 11 and 12** has been identified as different species of Nitrogen. This conclusion was verified by experimental testing using the parallel plate reactor and comparing the spectra for pure nitrogen versus air - the results of which are shown in **figures 13 and 14**.

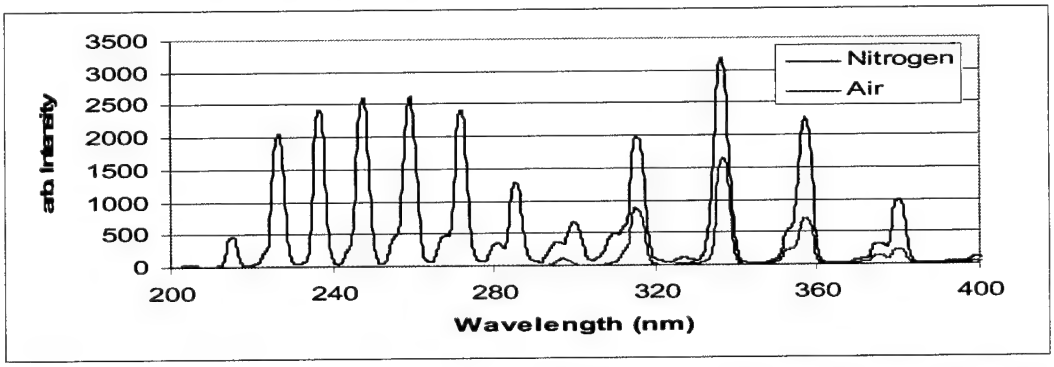

Figure 13. Comparison of UV spectra of pure Nitrogen to Air in the PPR3. (9kV and 9kHz)

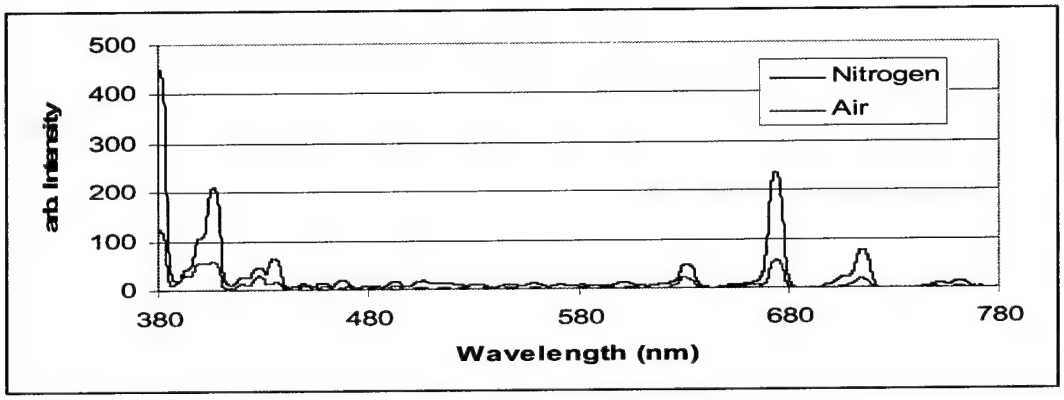

Figure 14. Comparison of the Visible Spectra of pure Nitrogen to Air in the PPR3 (9kV & 9kHz)

The conclusion that can be drawn for the two figures shown above is that within the resolution of the spectrophotometers, the observed spectra are most likely due to the nitrogen present in air.

An infrared detector has been integrated into the devices also. To date, significant emission information has not been obtained in this region up to the 1180 nm wavelength we could observe. The literature suggest that there are strong spectral emission for other species other than nitrogen further into the infrared – i.e. 1270 nm is reported to be the emission line for delta oxygen.

5.1.3 Direct Measurements of Particular Gases and Temperature

Some aspects of the plasma exhaust chemistry are easily measured with dedicated instruments. In particular, measurements of ozone, NO_2, and temperature are easily obtained with standard measurement devices. The following subsections show trends on these items for various plasma settings.

5.1.3.a Ozone Measurements

Figures 15 and 16 show ozone generation under two identical situations using Test Device 8 operating at various air feed flow rates and applied voltages, but at different frequencies. The ozone concentration (ppm by volume) was monitored 2 inches from the end of the plasma device. In general, higher flow rates reduce the ozone concentration levels. As noted in **Figures 16 and 17,** the amount of ozone produced increases with higher voltage level and frequency. Whereas, the rate of increase of ozone generation is largely insensitive to voltage at higher frequency, yet it is very sensitive at lower frequency.

Ozone generation in air plasmas is known to be a function of the distance between electrodes (and thus plasma volume), or gap, as it is referred to in the OAUGDP. The Test Device 8 has a gap size of 1.25 mm while the Test Device 10 has a gap size of 1.8 mm. Further, it is noted that an increase in ozone generation is created with a decrease in gap spacing. Also, frequency plays a much larger role in ozone generation as shown in **Figure 18**.

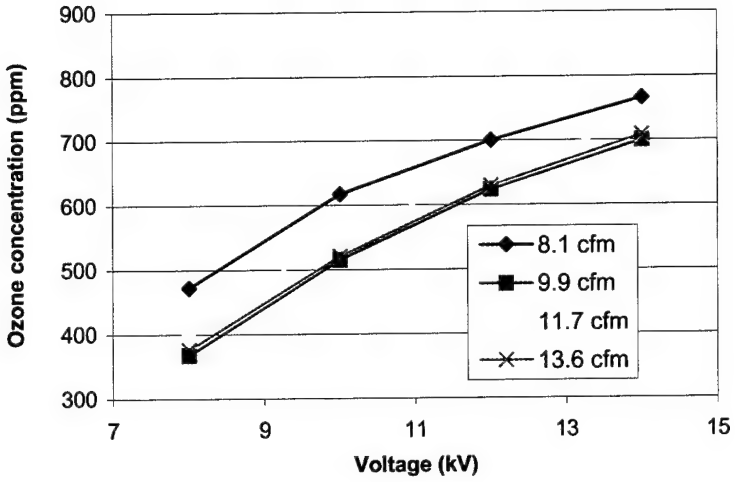

Figure 16. Ozone concentration in 2 kHz-plasma exhaust as a function of voltage. (ref. exp. 6,7)

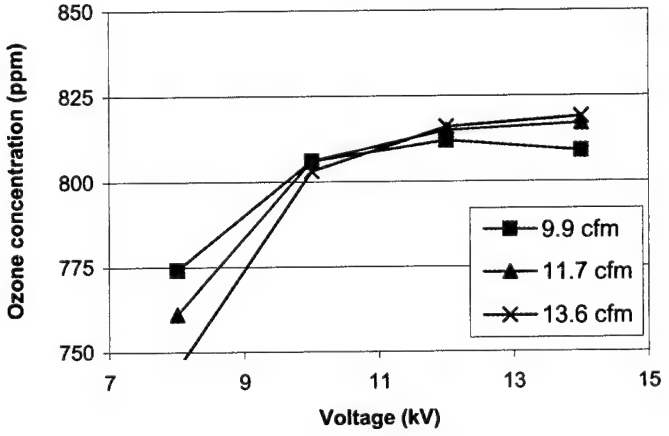

Figure 17. Ozone concentration in 6 kHz-plasma exhaust as a function of voltage. (ref. exp. 8,9)

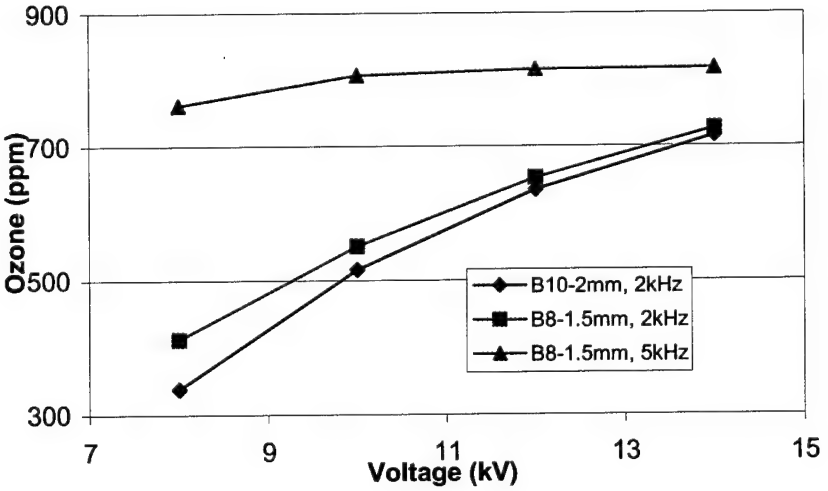

Figure 18. Ozone generation as a function of gap spacing and frequency. (ref. exp. 6,7,8,9)

5.1.3b NO_2 Measurement

Other well-known gas products of air generated-plasmas are nitrogen-oxygen compounds, in particular, NO and NO_2. A NO_x analyzer was interfaced with the plasma reactor exhaust to monitor NO and NO_2 liberation. Information on NO generation within the plasma and/or in the exhaust chemistry is not readily available because of the reaction of NO with ozone. NO and O_3 react according to the following:

$$NO + O_3 \rightarrow NO_2^* + O_2$$

$$NO_2^* \rightarrow NO_2 + h\upsilon$$

Because of the relatively high concentrations of ozone, NO is consumed and readily converted to NO_2 within the plasma. Measurements of the particular wavelength of light emitted by the second reaction may enable the determination of NO generated.

NO_2 generation as a function of voltage for a plasma reactor running at 2 kHz and 6 kHz is shown in **Figure 19**. Each data point was taken at 3 minutes of plasma generation. Further analysis (**Figure 20**) has shown that NO_2 concentration in the exhaust chemistry continues to increase with time of reactor operation. Upon shutdown of the plasma reactor, NO_2 concentrations continue to increase for approximately 1½ minutes, then decrease extremely slowly, back to original background values. It has been confirmed that absorption of the NO_2 on the acrylic walls of the sampling container and/or sample tube lines is most likely occurring. Therefore, the NO_2 measurements can be used qualitatively only.

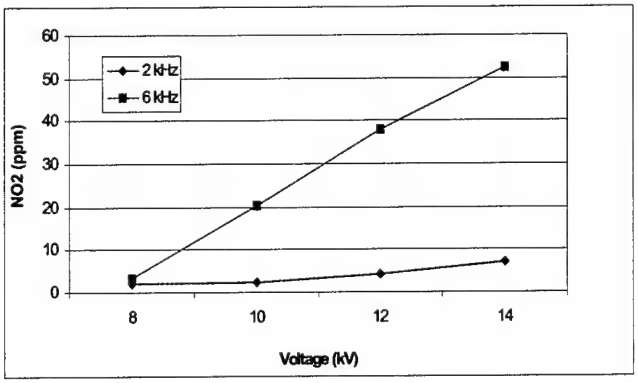

Figure 19. Nitrogen dioxide in plasma exhaust from APD 210 Test Device 8 at different frequencies (air flow = 11.7 cfm). (ref. exp. 6,8)

Based on the data collected at the lower and higher frequencies, NO_2 generation does not appear to be closely linked to airflow rates (not shown graphically), however, higher frequency power input generates significantly more quantities of NO_2 (**Figure 16**). As demonstrated in **Figure 17**, a steady state or equilibrium concentration of NO_2 does not seem to have been reached by 15 minutes of plasma operation; however, the rate of NO_2 production decreased with increasing operational time and can be assumed to reach an equilibrium concentration at some time >15 min. Again, absorption and thus desorption from the walls of the containers plays a role in the NO_2 balance and has not been accounted for.

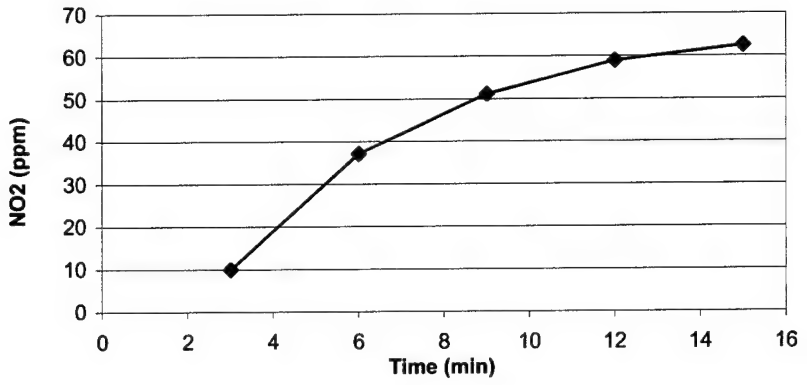

Figure 20. Nitrogen dioxide in 5 kHz, 12.8 kV plasma exhaust (air flow = 11.7 cfm). (ref. exp. 10)

5.1.3.c Temperature Measurements

OAUGDP exhaust chemistry temperature has been shown to play a role in the inactivation of microorganisms. It is important to note that it is not heat alone generating the killing results. Instead, it is likely the increase in temperature is favorably altering the kinetics of the chemical reactions generated by OAUDGP. Further discussion on this interaction is given in **Section 5.2 Biological Inactivation Results**. It is also important to note that OAUGDP exhaust chemistry temperatures are highly dependent on voltage, frequency, flow rate, gap size and device length (which determines the volume of plasma made). Higher exhaust chemistry temperatures are directly proportional to higher voltage, higher frequency, and/or larger plasma volumes. **Figure 21** shows the temperature dependency on voltage, frequency, and plasma volume (Test Device 8 vs. Test Device 10).

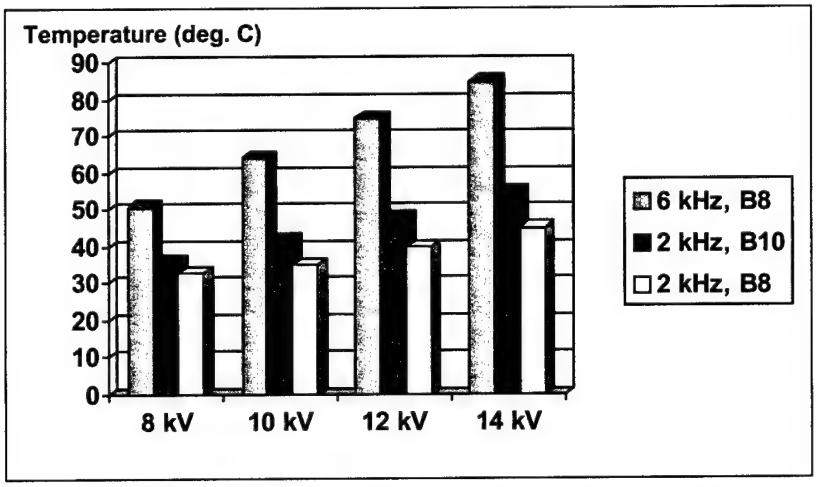

Figure 21. Temperature of plasma exhaust gas as a function of applied voltage for APD210 Test Device 8 (1.25 mm gap) and APD210 Test Device 10 (1.8 mm gap, larger plasma volume) at different frequencies.

5.2 Efficacy Studies to Evaluate Variables of APD 210 Test Devices.

To accurately measure the efficacy of OAUGDP to decontaminate materiel tainted with biological contaminants, bacterial endospores not vegetative bacterial cells were used. This is due primarily to the physiological makeup of endospores and their overall resistance to neutralization by any means. Although AGT has used all types of microorganisms in its research and development of the OAUGDP, it traditionally uses endospores to measure the efficacy of the OAUGDP as a decon device.

A number of experiments have been performed by AGT to demonstrate the neutralization ability of direct plasma delivery and an example is shown in **Figure 22**. As shown in **Figure 22**, five million anthrax endospores are inactivated in 100 sec. Also as shown, when OAUGD plasma is operated with increased concentrations of oxygen there is a dramatic decrease in neutralization times such that five million spores are inactivated in approximately 53 sec. This data strongly suggests different active species or different concentrations of active species are significant when samples are immersed in plasma as well as localized physical factors such as UV and ion bombardment have important roles in reducing the number of endospore survivors.

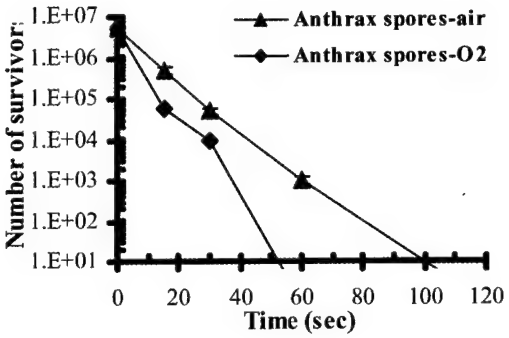

Figure 22. Efficacy of the APD 210 device against *B. anthracis* endospores.

Because of the somewhat limited applicability of direct plasma delivery systems for military decon, AGT has developed several indirect plasma systems including the APD 210 which delivers active species to a sample in a remote location. As shown in **Figure 23a,** the samples inoculated with 10^7 anthrax spores were inactivated within three minutes when placed 2 inches downstream of the distal end of the APD 210 device. During the process of APD 210 development as a potential decontamination device, AGT has shown neutralization of endospores including anthrax when the samples were located 16 in or 16.6" away from the distal end of the APD 210 device (**Figure 23b**). In this operating regime the time necessary for inactivation is about 6 minutes. The operating variables required for this OAUGDP performance is 13kV, 8.6kHz with airspeed of 4800 fpm.

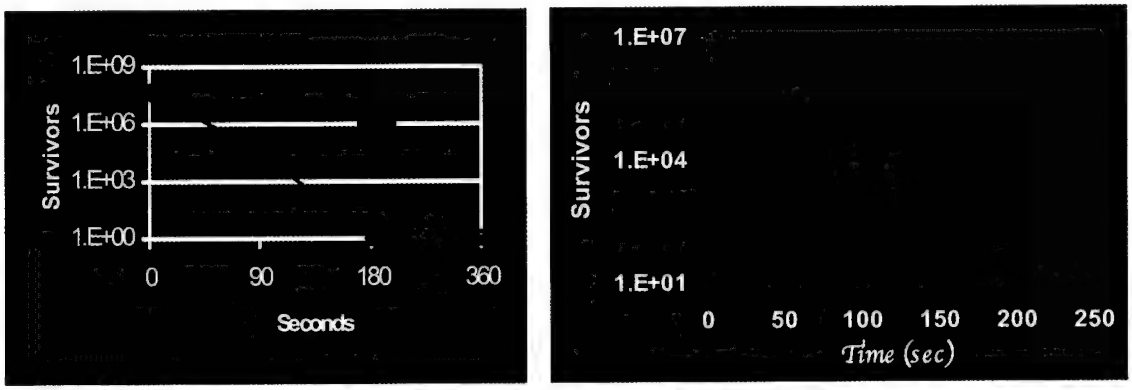

Figure 23. APD 210 efficacy against anthrax endospores.

For valid applications in decontamination, AGT has untaken the task of developing a test device which encompasses the optimum operating variables of power, airspeed, gap distance in order to deliver the most efficient and efficacious device. To optimize the APD 210, AGT is elucidating the chemistry of the plasma that efficiently neutralizes microorganisms.

5.2.1 Experimental results of biological inactivation during the study.

Typically when a OAUGDP variable is modified its effect is evaluated by determining changes in efficacy. Below is a discussion of results focusing on known OAUGDP variables and their effect on

efficacy. In the first section, discussion will be presented based upon the type of APD 210 test device used. In the subsequent section, an overview of OAUGDP variables and relationships and their effect on efficacy will be presented. Key points to be noted in measuring certain variables are all ozone concentration reported are the last ozone concentration measured (at max time) unless otherwise noted. All temperatures are the highest temp recorded at maximum time unless otherwise noted.

5.2.1a APD 210 Test Device 8. The attributes of Test Device 8 are described in Table 2. Essentially the Test Device is 55.56 cm in length with a 1.25 mm gap between the electrodes and the inner electrode is composed of 316 stainless steel while the outer electrode is Pyrex. This Test Device was used early in project and suffered irreparable damage in early December and Test Device 10 was fabricated. The initial experiments performed with Test Device 8 were focused on varying the temperature and fixing the voltage, frequency and airflow as shown in **Table 6**. Ozone and NOx were not monitored in the very early experiments. The next set of experiments performed with Test Device 8 looked at the role of altering voltage which subsequently increased the temperature of the OAUGDP exhaust. The data shows that with increased temperatures the neutralization rate increased. Also, when the voltage was increased from 12 kV to 14 kV a rise in plasma exhaust temperature as well as the rate of neutralization was increased. More extensive tests were not performed with this test device.

Table 6. Results of Test Device 8 testing.

Exp #	Sample Location	Voltage kV	Freq. kHz	Airflow CFM	Time min	Temp °C	Log reduction
II122	2"	12	5.4	0.6	12	63	<1
II115-9	2"	12	5.4	0.6	16	69	>5
II110-14	2"	14	5.4	0.6	16	79	4
II109	8"	14	5.4	0.6	16	82	4

Note: The average untreated samples contained 2.3 e6 endospores
Later experiments with Test Device 8 began to show inconsistency in the data and failed shortly afterwards.

5.2.1.b **APD 210 Test Device 10.** The attributes of Test device 10 are described in **Table 2.** Essentially the Test Device is 57.15 cm in length and 2.8 mm gap between the electrodes and the inner electrode is composed of 316 stainless steel while the outer electrode is Pyrex. This primary difference between Test Device 8 and 10 is the later has an increase in the gap (distance between the electrodes) of 1.55 mm. A series of Test Device 10 variables were altered and the effect on efficacy was examined. The variables examined included changes in airflow, voltage, frequency, temperature, distance of the sample from the distal end of the test device, and time. AGT is cognizant of the interdependence of some of these variables but has tried to isolate certain ones to study their contribution in neutralization of microorganisms. The initial experiments performed with Test Device 10 were to examine the role of airflow upon neutralization rates. As shown in **Table 7**, preliminary experiments indicated a trend of increasing airflow through the test device caused a decrease in neutralization efficiency. A putative explanation for this observation is the increased airflow diminishes dwell time of the active species on the biological sample or the interaction time between the active species. Further experimentation demonstrated complete neutralization of endospores occurred when exposed the OAUGDP exhaust at different airspeeds (10-16 CFM) with an operating regime of 13.8kV, 5.8kHz, 2 inches from the distal end of the device, with ozone levels reaching approximately 794 ppm and NOx levels 60 ppm. The temperature of the exhaust gas was between 90-100°C. This data indicates the operating regime reached a threshold which compensates any negative effects of increasing airflow such as decreased dwell time of the active species.

Table 7. Results of Varying the Airflow of Test Device 10 upon Efficacy.

Voltage kV	Freq. kHz	Airflow CFM	Time min	Temp °C	Ozone (ppm)	NOx (ppm)	Log reduction
12.8	5	11.7	12	79	827	58	≥5
12.8	5	13.6	12	79	828	59	3
12.8	5	11.7	15	77	829	63	≥5
12.8	5	13.6	15	79	830	55	4

The second set of experiments using Test Device 10 evaluated the role of increased voltage and lower frequency (16kV, 2kHz). The results of these experiments are shown in **Table 8**. In general, under this operating regime the neutralization rate was diminished significantly. It should be noted that the ozone and NOx levels were elevated. Furthermore, the temperatures were elevated except when it was purposefully reduced and no significant differences in efficacy were seen. Therefore, this operating regime produces significant levels of ozone and NOx and temperatures but unlike the operating regime presented in **Table 7** there is not a significant level of inactivation of endospores. This trend could be associated in part to different reactive chemistry being produced with lower frequencies.

Table 8. Representative Results When the Voltage and Frequency

Voltage kV	Freq. kHz	Airflow CFM	Time min	Temp °C	Ozone (ppm)	NOx (ppm)	Log reduction
16	2	10	15	70	827	58	≤2
16	2	10	15	75	749	40	≤1.5
16	2	10	15	72	793	43	0.5
16	2	10	15	56	830	38	0.5

At this point in the study, we have determined a functional operating regime for the APD 210 Test Device 10 therefore the next set of experiments was done to evaluate the role of plasma exposure time on neutralizing *B subitils var niger* endospores. The plasma operating conditions were as follows: 12kV, 5.8kHz, 10 cfm, with samples 12 inches away from the distal end of the APD 210 device. Two temperatures regimes were used. The temperatures of the plasma exhaust were measured with thermocouples located at the location of the samples. The lower temperature was 45-55°C while the higher temperature was 75-85°C. As shown in **Figure 24**, the initial inoculum was 2e6 and when the APD 210 Test Device 10 was operated in the lower temperature regime, no significant reduction of endospores was noted with exposure times from 1 9 min. However, in the higher temperature regime neutralization occurred within 5 min and no survivors were detected even with a 72-96 hr incubation period.

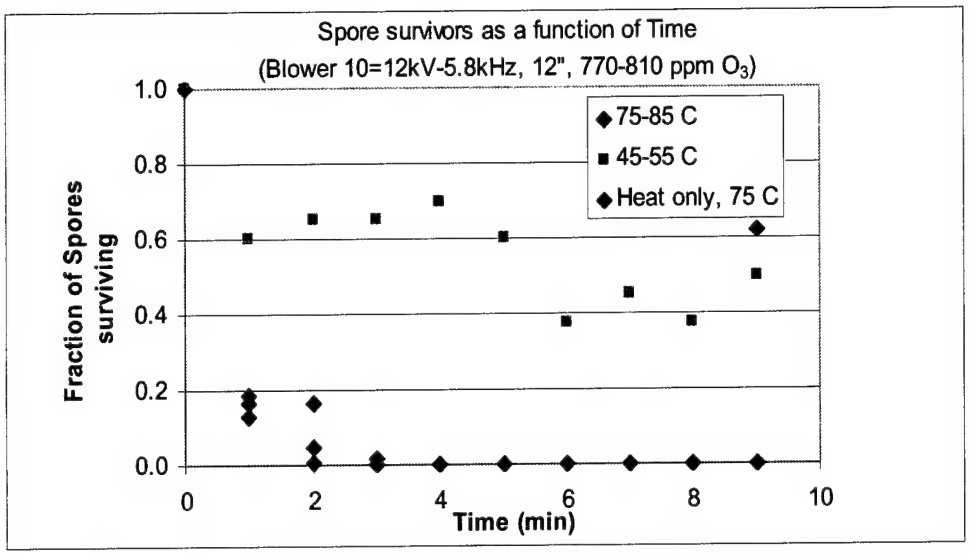

Figure 24. Endospore survivors as a function of time .

Figure 25 shows representative experiments performed with Test Device 10 focusing upon the role of temperature. For all data points the fixed operating regime was 12 kV, 5.8kHz, 10 CFM, 12 min exposures, sample placement was 12 inches away from the distal end of the device. The temperature was controlled by heating the airstream prior to entering the Test Device 10. From the representative data there appears to be effective neutralization. It is important to note that the temperature recorded was taken at the end of test run, therefore it is the maximum temperature. A period of 2-3 min was necessary to reach maximum temperature. These results show a correlation between temperature of the OAUGDP exhaust and neutralization rate. Control experiments were performed with heat only for up to nine minutes and no neutralization occurred with the endospores. Elevated temperatures are related to increases in the kinetics of reactions and more efficacious active species are generated at the described operating regime.

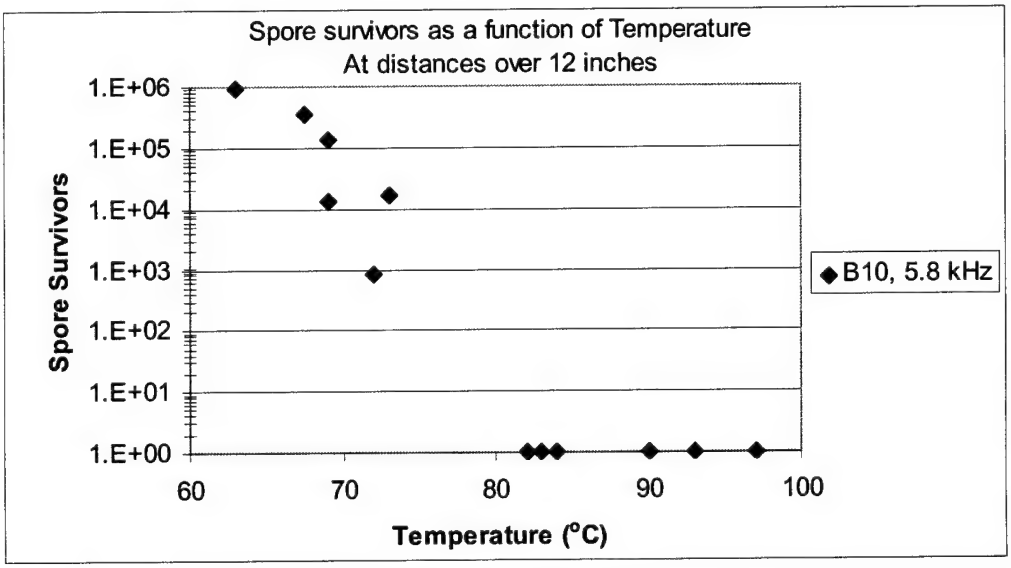

Figure 25. Endospore survivors as a function of temperature.

5.2.1.c APD 210 Test Device 11 The attributes of Test Device 11 are described in **Table 2** and was optimized based upon an analysis of experimental data performed during the first several months of

this work effort. The test device is only 14.61 cm long and has a 1.25 mm gap between the electrodes and the inner electrode is composed of 316 stainless steel while the outer electrode is Pyrex. This device is far more efficient to operate and was fabricated and used during the last two weeks of the effort. The important finding from these experiments was the rate of neutralization using similar variables was equivalent to the larger more power demanding APD 210 Test Devices 8 or 10. The data presented in **Figure 26** shows the relationship between frequency and temperature. When the frequency is increased the temperature also increases and more importantly certain active species (to be identified in the Phase II effort) are generated that effectively neutralize endospores. The ozone concentration was less than 70% of the amount measured in Test Device 10. Interesting, when the frequency was adjusted to 5.8 kHz the neutralization rate was the same but the ozone concentration was only 400 ppm and the NOx is less than 15ppm. The NOx values are viewed qualitatively because of adsorption and desorption on the acrylic walls of the test chamber.

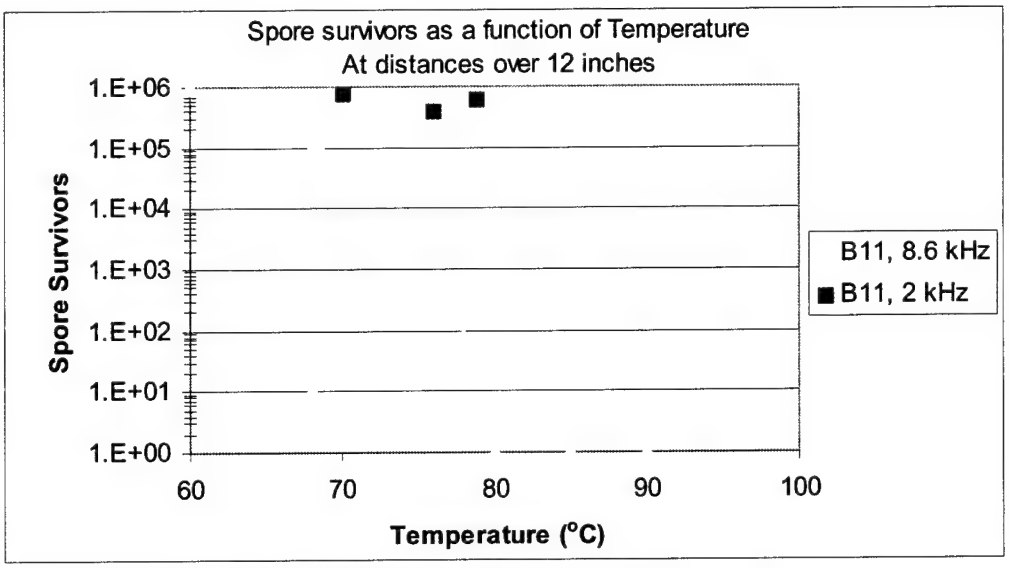

Figure 26. Endospore survivors as a function of temperature.

During the course of this work effort AGT has made a significant advancement in reducing the power requirement and levels of ozone and NOx in Test Device 11. This finding is a first step in developing an efficient decontamination tool for use on materiel.

6. Conclusions

The work performed under this contract focused on developing and initiating a study to identify active species generated by OAUGDP™ that are primarily responsible for the inactivation of microorganisms. For this project, AGT used the APD 210 (Atmospheric Plasma Device), which has been proven capable of neutralizing both biological and chemical warfare agents as well as simulants without negatively affecting sensitive equipment. The aims of the Phase I STTR have been met and the success of this effort will be used as a platform for the more comprehensive Phase II effort. The long term goals are to identify OAUGDP generated active species responsible for destroying microorganisms, and develop OAUGDP device to decontaminate biological and chemical warfare agents.

Under this contract, AGT focused on fabricating test devices and interfacing them with diagnostic equipment. We also began the task of identifying variables driving the OAGUDP exhaust chemistry. Some of these variables included: frequency, voltage, airflow, time, type of microorganism, sample location, and temperature of exhaust. It was found temperature (measured at the sample location) plays a role in the kinetics of the gas exhaust and was found to have an effect on spore decontamination. In many instances, when the exhaust temperatures reached 75°C or higher, 10^6 log

killing was achieved, while lower inactivation was demonstrated at temperatures lower than 75°C. It is important to note that temperature is couple with other variables because temperature alone (in the exhaust range) does not induce killing, as demonstrated by maintaining an exhaust temperature of 75°C for 15 min as shown in **Figure 27.**

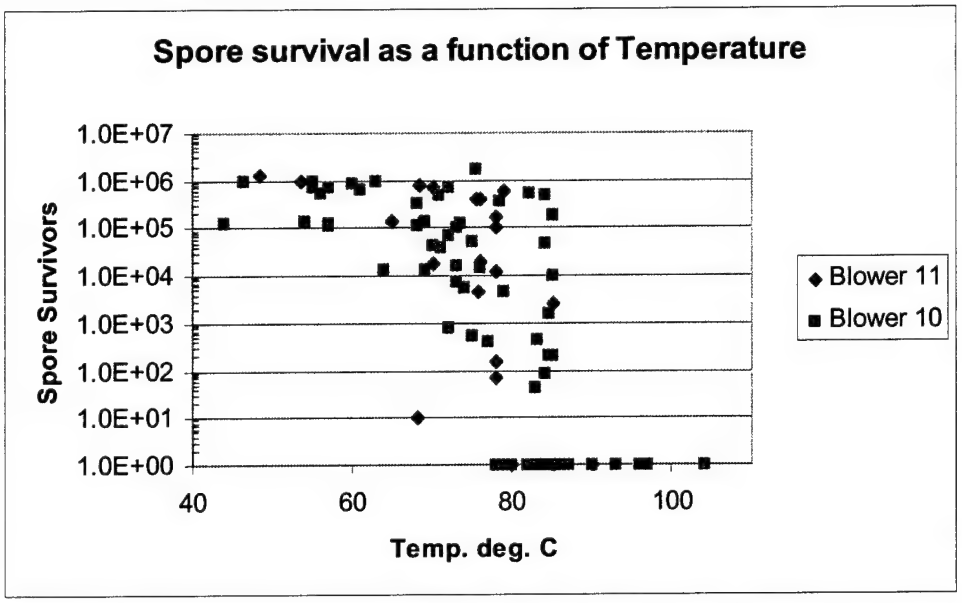

Figure 27. Summary of data of endospores survival as a function of temperature.

Frequency: Earlier results have indicated that neutralization of microorganisms was dependent upon a threshold frequency level. In this work effort similar results were found. For instance, operating at temperatures above the 75°C threshold, less than 2 logs of killing was obtained when the frequency was low (2 kHz). However, 5 logs of neutralization were attained at frequencies above 5kHz as described in **Tables 6 and 7.**

Ozone: There is some correlation between ozone concentration and neutralization in frequency operation above 5.4 kHz. However, in experimental data taken at lower frequency and high ozone concentrations (750-800 ppm O3 which corresponds to 0.13 wt% at the typical flow of 10 cfm), and with temperatures above the 75°C threshold, less than 2 logs of inactivation was obtained, pointing to some as yet undetermined species or synergistic effect acting in the spore destruction as shown in **Figure 28.**. Speculation as to the role of singlet delta oxygen, a long-lived, excited state of molecular oxygen, will be pursued in the Phase II contract. The theory that singlet delta oxygen has a role in the biological destruction is supported by:

- A life-time long enough that, at our standard air flow rate of 10 cfm, supports its existence at up to a few feet from the end of the plasma. (ref.)
- The correlation between killing at higher frequency, but not as efficiently at lower frequency. It is possible that singlet delta O_2 created at higher frequency (above 5.4kHz) and not in significant quantities at lower frequency.

A summary of data showing ozone concentrations is shown in **Figure 29.**

Flow rates: were shown to have a significant effect on killing, as seen in **Table 6**. Several experiments were completed under identical flow conditions ***into*** the reactor, same temperatures, identical voltage and frequencies. However, in one case the flow ***as it exited the reactor*** was diffused prior to reaching the sample through the use of a screen. Note that the pathway the gas followed was not lengthened, but the "plume" was diffused, and much lower kill rates were obtained. Therefore, a moving flow is needed to obtain successful decontamination, but does not appear to be a sensitive parameter. This would suggest active specie(s) that is present in low concentrations.

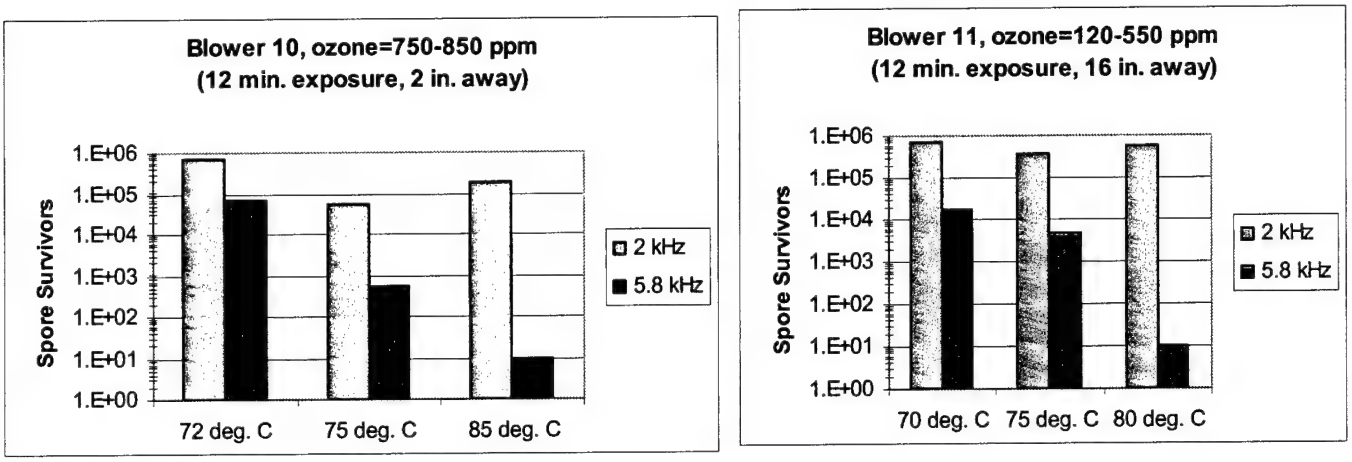

Figure 28. Spore survival as a function of ozone concentration.

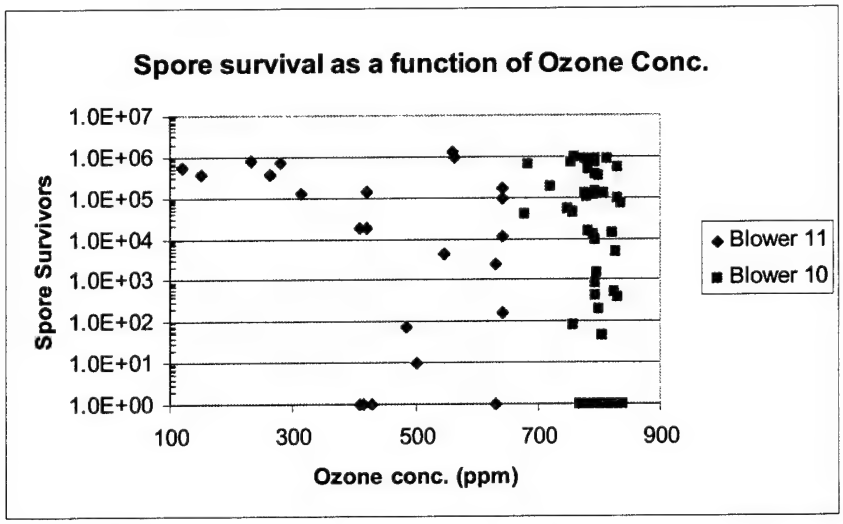

Figure 29. Summary of endospores survival as a function of ozone.

UV/vis spectra: were obtained within the plasma. The majority of the emission peaks were identified as excited states of nitrogen. This was verified by running pure nitrogen plasmas. This phenomenon was also noted by Gomez, et. al. In the UV region below 297 nm, ozone absorbs large amounts of UV. (Ref. Herzberg) Because of this characteristic of ozone, we may safely assume that UV would not play a significant role in decontamination within the plasma, since the most energetic photons are absorbed by the ozone. Clarification of the spectra, and separation of peaks, can be made with more sensitive spectroscopy equipment as is proposed in the Phase II scope.

Infrared and Raman spectra: will be obtained in the Phase II contract. Singlet delta oxygen is most frequently measured in the IR region for which no data has yet been collected.

NO and NOx: any effects of NO toxicity on microorganisms in the plasma exhaust are likely ruled out because of the conversion of NO to NO_2 via reaction with O_3. Monitoring of the plasma exhaust at the sample location showed lower than detectable levels of NO present with the exception of the very lowest concentrations of O_3 measured (< 150 ppm) in which case there was much lower destruction of the spores as well. NO_2 concentrations in the exhaust do not appear to correlate with biological decontamination as shown in **Figure 30**. Some uncertainty in this data exists because the NO_2 is known to adsorb onto the acrylic walls of the sample chamber. Therefore this data was evaluated

qualitatively not quantitatively. During Phase II a glass sample chamber will be used, thereby removing this uncertainty.

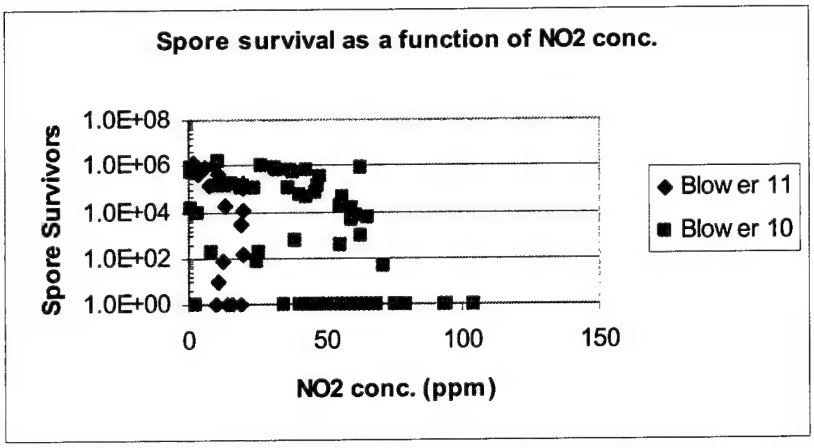

Figure 30. Bacterial endospores survival as a function of No_x concentrations.

Initial testing using the HPR-60 substantiated the presence of excited states (or fragmentations from irregular species) of NO, O, and NO_2 in the plasma exhaust relative to background scans of electron energies. Further investigations into the presence of excited state species will be made with the HPR-60 EQP analyzer.

6. REFERENCES

1. Kitayama, J. and M. Kuzumoto, "Analysis of Ozone Generation from Air in Silent Discharge", J. Phys. D: Appl. Phys. (32) 1999.

2 Laux, C. O., et. al. "Ionization Mechanisms in Two-Temperature Air Plasmas", Published by American Institute of Aeronautics and Astronautics. AIAA 99-3476. 1999.

3 Packman, D. M. et. al., "Meaurement and Modeling of OH, NO, and CO_2 Infrared Radiation in a Low Temperature Air Plasma" Published by American Institute of Aeronautics and Astronautics. 1999.

4 Ono, R. and T. Oda, "Measurement of Hydroxyl Radicals in an Atmospheric Pressure Discharge Plasma by Using Laser-Induced Fluorescence", IEEE Trans. on Industry Applications, (36) 1, Jan/Feb. 2000.

5 Grossweiner, L. "Singlet Oxygen: Generation and Properties" http://www.photobiology.com/educational/len2/singox.html Feb 2003.

6 Jeong, J. Y., et. Al. "Etching Polyimide with a Nonequilibrium Atmospheric-Pressure Plasma Jet", J. Vac. Sci. Technol. A 17(5), Sept/Oct 1999.

7 Gomez, S. et. al. "Spectroscopic Characterization of an Atmospheric Pressure Glow Discharge", Department of Pure and Applied Physics, The Queen's University, Belfast BT7 1NN.

8 Herzberg, Molecular Spectra and Molecular Structure, Second Ed., D. Van Nostrand Co., Inc., New York, 1950.

Appendix 1. Microwave Diagnostics of the OAUGDP

The following section is based upon a report of activities performed at the UT Plasma Sciences Laboratory led by Professor J. Reece Roth and prepared by Mr. Y. Yang and Prof. M. Howlader. The purpose of the Phase I subcontract with the UT Plasma Science Laboratory was to utilize a microwave network analyzer to determine both the electron number density and electron collision frequency for a OAUGDP device.

The testing system was altered from the original flat plasma configuration to test a fluorescent light tube (60 Hz – low pressure glow discharge). Initial testing of UT's parallel plate revealed that the instrumentation didn't have enough sensitivity. This will be performed under the Phase II work effort.

Theory Background: Appleton's Equation

When an electromagnetic plane wave propagates in a homogeneous unmagnetized plasma, the complex index of refraction is given by *Appleton's equation,*

$$\bar{\mu}^2 = (\mu - j\chi)^2 = 1 - \frac{\omega_{pe}^2/\omega^2}{C_1 \pm C_2^{1/2}}, \qquad (1)$$

where, C_1 and C_2 are constants, and ω is the incident frequency with unit radian. The term ω_{pe} is the electron plasma frequency given by,

$$\omega_{pe} = \left(\frac{n_e e^2}{m_e \varepsilon_0}\right)^{1/2} (rad/s), \qquad (2)$$

Derived from Appleton's equation, the attenuation as a function of plasma variables and incident frequency is,

$$dB = 10\log_{10}\left\{\left(\frac{E}{E_0}\right)^2\right\} = 10\log_{10}\left(e^{-\frac{2d}{\delta}}\right) = 10\log_{10}\left(e^{-\frac{2d\omega}{c}\chi}\right) = f(n_e,\ v_c, \omega, d) \qquad (3)$$

The Phase shift as a function of plasma variables and incident frequency is,

$$\Delta\varphi = \varphi - \varphi_f = \left(\frac{\omega}{c}\mu - \frac{2\pi}{\lambda}\right)d = g\left(n_e,\ v_c,\ \omega, d\right) \qquad (4)$$

In the above two equations d is the propagation distance through plasma, n_e is the electron number density, v_c is the electron collision frequency, and ω is the frequency of the incident electromagnetic wave.

Schematic for Experiment Setups

Figure A-1 shows the measurement system, which includes the TTL signal generator, the network analyzer and the plasma. **Figure A2 (a and b)** demonstrates the experimental setup for a test case – a standard fluorescent light bulb. **Figure 3 (a and b)** depict the tested arrangement for the experimental setup for a parallel plate reactor.

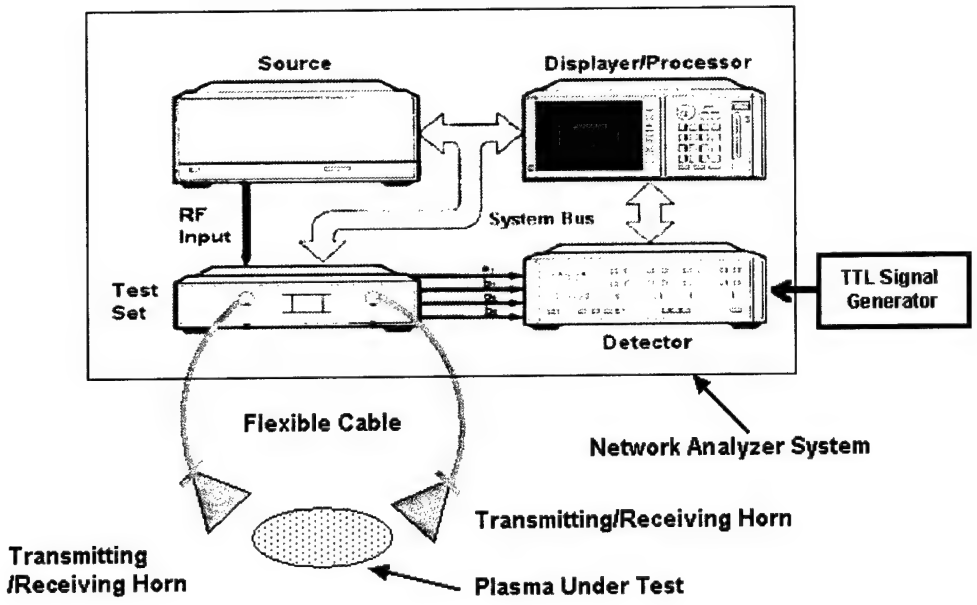

Figure A 1: General Measurement System Diagram

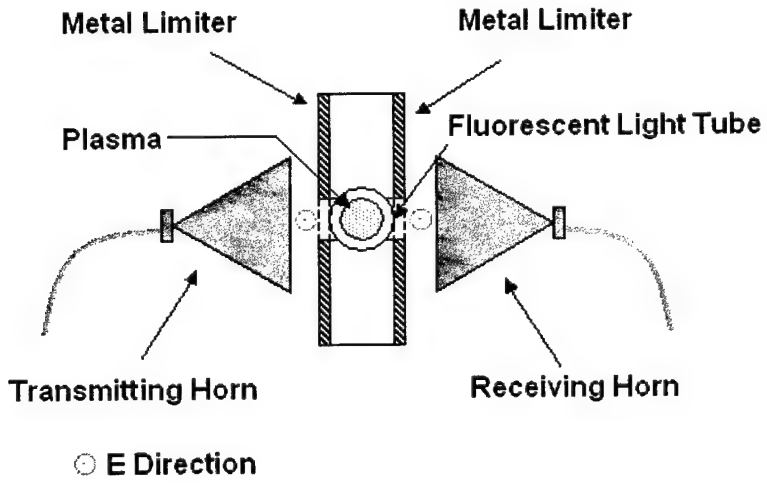

Figure A 2(a): Elevation of Fluorescent Light Tube Test Plasma

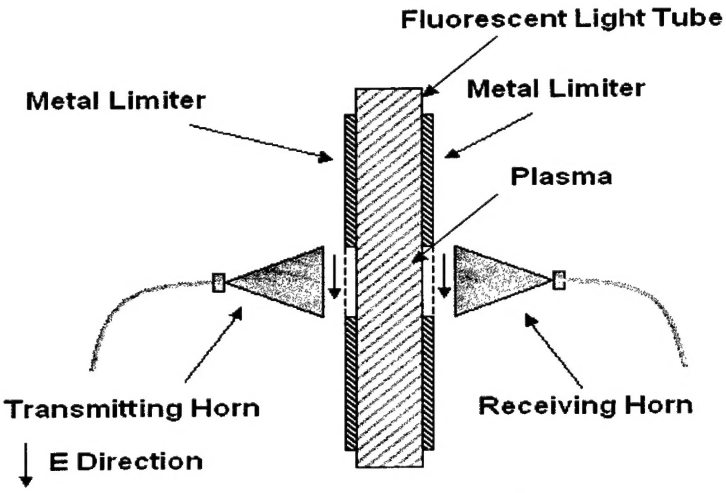

Figure A 2(b): Plan View of Fluorescent Light Tube Test Plasma

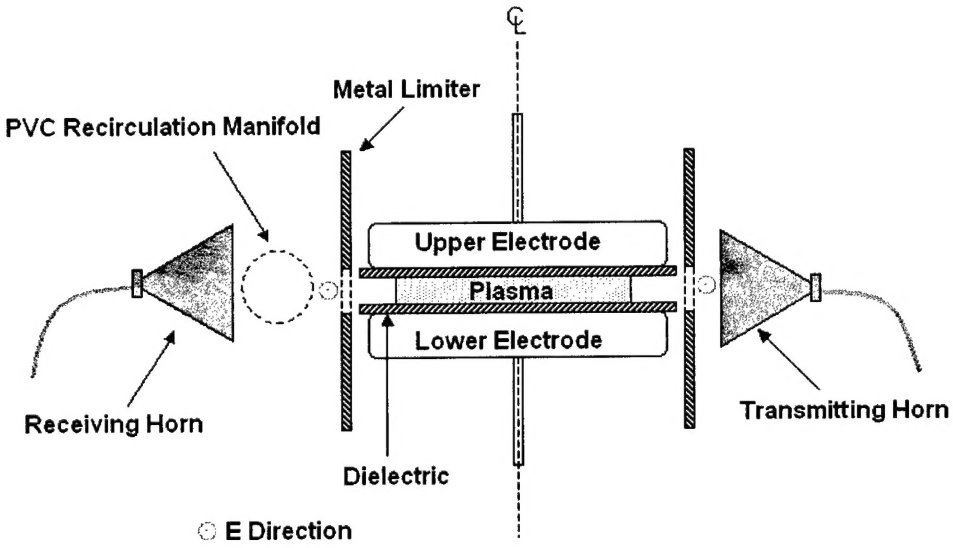

Figure A 3(a): Elevation of Parallel Plate Reactor

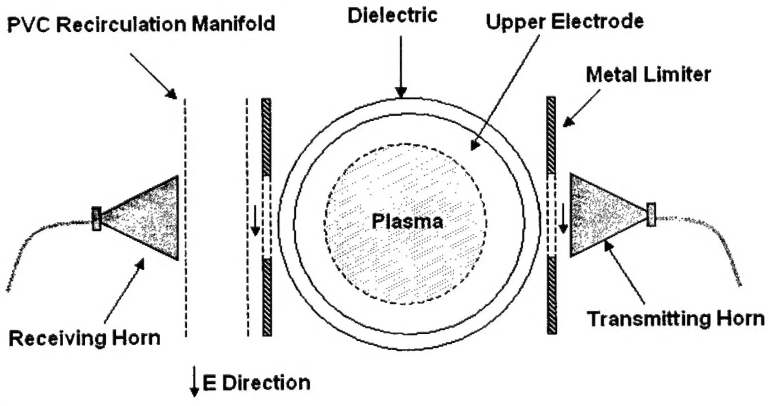

Figure A 3(b): Plan View of Parallel Plate Reactor

Time-resolved Experiment Result from Fluorescent Light Tube Measurement

The UT Plasma Lab measured the attenuation and phase shift value when a 15 GHz microwave propagates through a fluorescent light tube with 3.8 cm diameter. The fluorescent light was connected to the power line with 60 Hz frequency and 120 Vrms. Figure 4 shows the sampling points in one cycle when making time-resolved measurement. **Figures A 4 and A 5 and Table A 1** give the measured value of attenuation and phase shift, and the electron density and collision frequency derived from measured data.

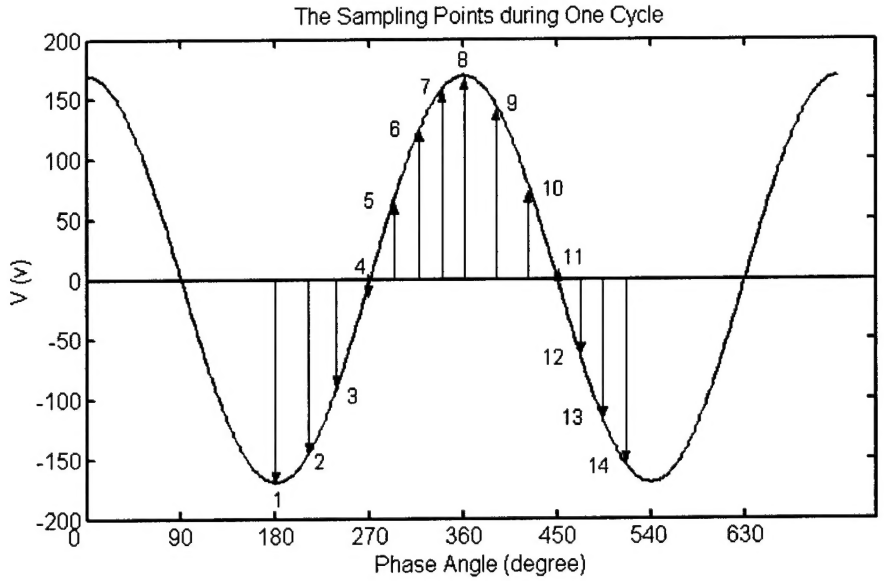

Figure A 4: Sampling Points

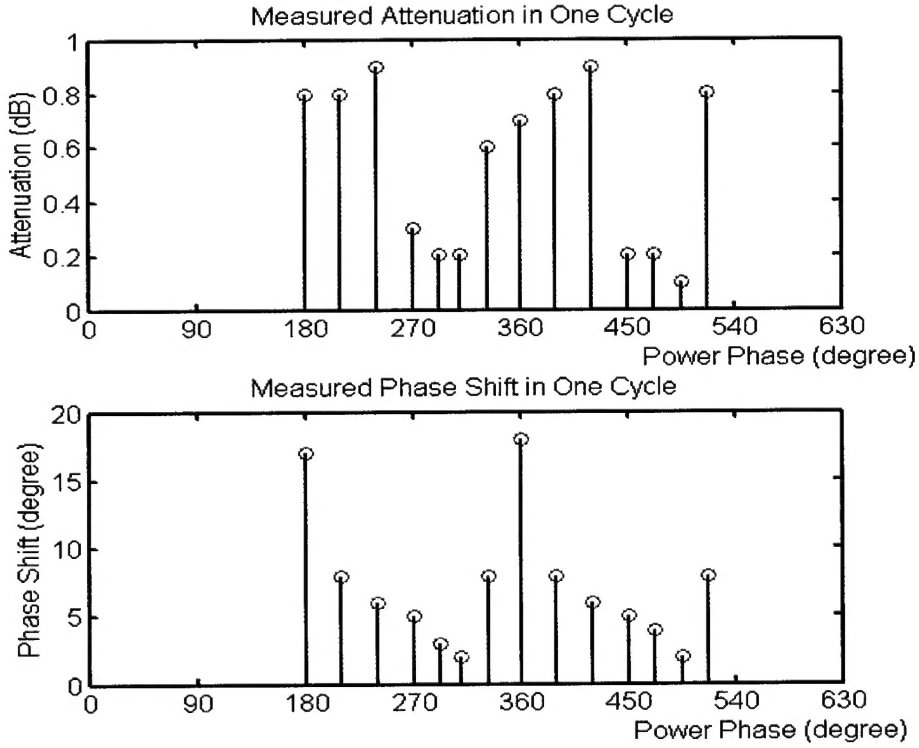

Figure A 5: Measured Data

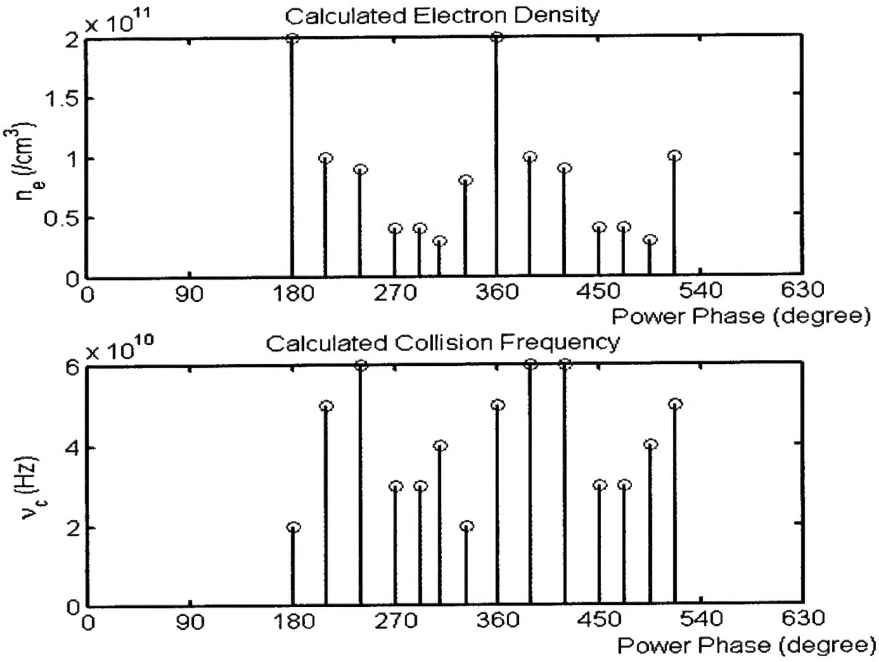

Figure A 6: Calculated Result

Table A 1: Measured Data as well as Derived Electron Density and Collision Frequency

Note: The error bars are ± 0.05 dB for measured attenuation and ± 1^0 for phase shift.

Sampling	180^0	210^0	240^0	270^0	292.5^0	310^0	332.5^0
Attenuation (dB)	0.8	0.8	0.9	0.3	0.2	0.2	0.6
Phase Shift (degree)	17	8	6	5	3	2	8
Electron Density (/cm^3)	2e11	1e11	9e10	4e10	4e10	3e10	8e10
Collision Frequency (Hz)	2e10	5e10	6e10	3e10	3e10	4e10	4e10

Continued Table 1:

Sampling	360^0	390^0	420^0	450^0	472.5^0	495^0	517.5^0
Attenuation (dB)	0.7	0.8	0.9	0.2	0.2	0.1	0.8
Phase Shift (degree)	18	7	6	5	4	2	8
Electron Density (/cm^3)	2e11	1e11	9e10	4e10	4e10	3e10	1e11
Collision Frequency (Hz)	2e10	5e10	6e10	3e10	3e10	4e10	5e10

Simulated Result for Fluorescent Light Tube Measurement

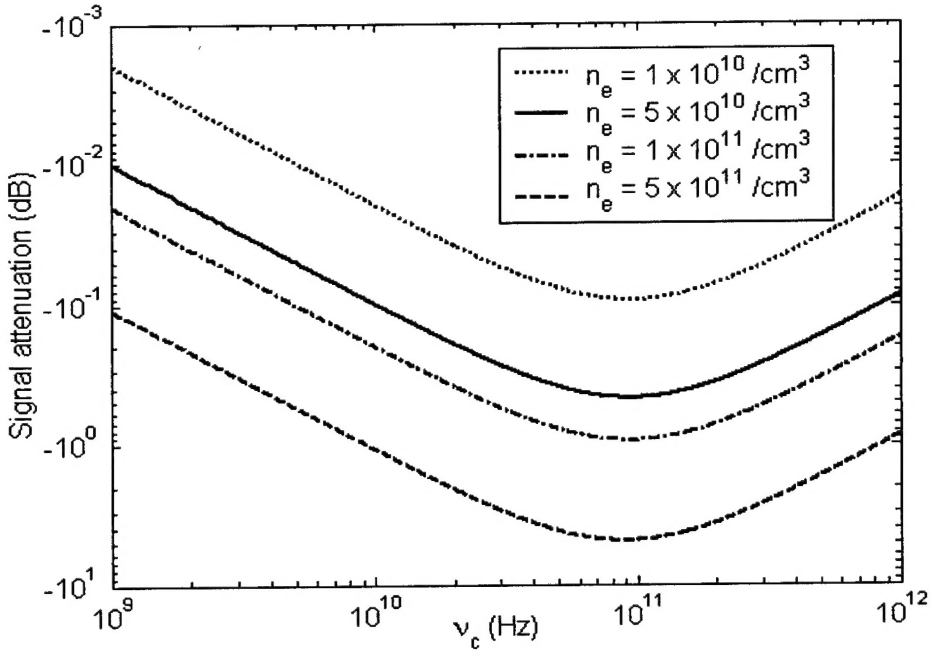

Figure A 7: Attenuation versus Collision Frequency

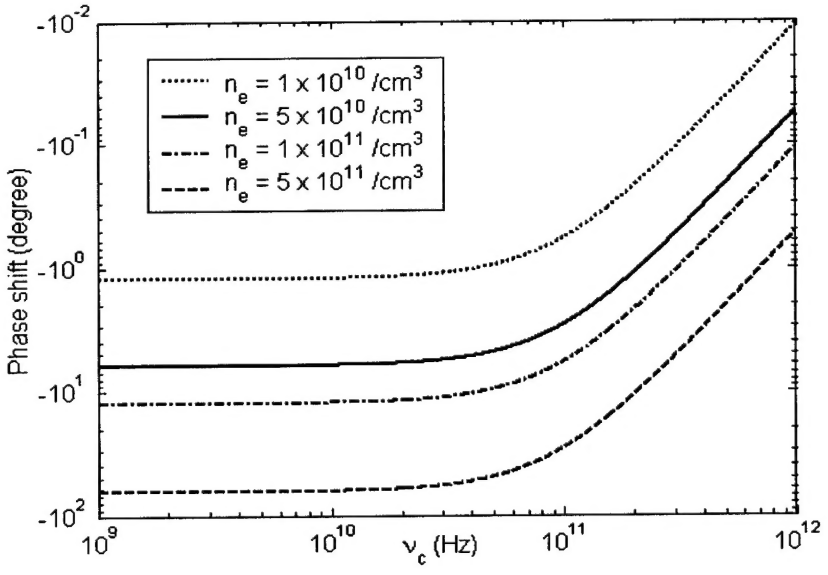

Figure A 8: Phase Shift versus Collision Frequency